

## CANADIAN THESES ON MICROFICHE

## THÈSES CANADIENNES SUR MICROFICHE



National Library of Canada  
Collections Development Branch

Canadian Theses on  
Microfiche Service

Ottawa, Canada  
K1A 0N4

Bibliothèque nationale du Canada  
Direction du développement des collections

Service des thèses canadiennes  
sur microfiche

### NOTICE

The quality of this microfiche is heavily dependent upon the quality of the original thesis submitted for microfilming. Every effort has been made to ensure the highest quality of reproduction possible.

If pages are missing, contact the university which granted the degree.

Some pages may have indistinct print especially if the original pages were typed with a poor typewriter ribbon or if the university sent us an inferior photocopy.

Previously copyrighted materials (journal articles, published tests, etc.) are not filmed.

Reproduction in full or in part of this film is governed by the Canadian Copyright Act, R.S.C. 1970, c. C-30. Please read the authorization forms which accompany this thesis.

### AVIS

La qualité de cette microfiche dépend grandement de la qualité de la thèse soumise au microfilmage. Nous avons tout fait pour assurer une qualité supérieure de reproduction.

S'il manque des pages, veuillez communiquer avec l'université qui a conféré le grade.

La qualité d'impression de certaines pages peut laisser à désirer, surtout si les pages originales ont été dactylographiées à l'aide d'un ruban usé ou si l'université nous a fait parvenir une photocopie de qualité inférieure.

Les documents qui font déjà l'objet d'un droit d'auteur (articles de revue, examens publiés, etc.) ne sont pas microfilmés.

La reproduction, même partielle, de ce microfilm est soumise à la Loi canadienne sur le droit d'auteur, SRC 1970, c. C-30. Veuillez prendre connaissance des formules d'autorisation qui accompagnent cette thèse.

**THIS DISSERTATION  
HAS BEEN MICROFILMED  
EXACTLY AS RECEIVED**

**LA THÈSE A ÉTÉ  
MICROFILMÉE TELLE QUE  
NOUS L'AVONS REÇUE**

**Canada**

Electron Detachment Cross-Section  
OF  
Bromine negative ions in ( He,Ne,Ar,,Kr and Xe )  
By  
Isam Ahmed Abbas

A thesis submitted to the School of  
Graduate Studies of the University  
of Ottawa in partial fulfilment of  
the requirements for the degree of  
Master of Science.

Department of Physics  
Faculty of Science and Engineering  
University of Ottawa

© Isam Ahmed Abbas, Ottawa, Canada, 1985.



UNIVERSITÉ D'OTTAWA  
UNIVERSITY OF OTTAWA

## ABSTRACT

.....

The cross sections for both the single and double electron detachment of  $\text{Br}^-$  ions when passed through thin rare gas targets has been measured between 10 keV and 100 keV under single collision conditions.

The single electron detachment cross sections show small energy dependence for all the targets but neon, where it is found to be energy independent. Small oscillations in Xe target were also observed beyond 30 keV energy.

Our experimental data for the system of  $\text{Br}^-$  and the He gas target has been compared with the Gauyacq's zero range<sup>12</sup>, it shows good agreement in the restricted energy range between 20 keV to 70 keV.

The cross sections for double electron detachment was found to have some dependence on energy in all gas targets.

### Acknowledgements

I would like to express my appreciation to my thesis supervisor, Dr. B. Hird for his suggestion of this avenue of research and for his help and guidance in performing the experiments and interpreting the results.

Also, I would like to thank Mr. C.N. Goodchild and his other technical staff for their assistance in the construction of the apparatus.

I am much thankful to the Government of IRAQ for their constant support in completing this degree successfully.

Finally, special thanks to my parents and my brothers for their encouragement.

**TABLE OF CONTENTS**

.....

Abstract .....	I
Acknowledgements .....	II
Table of Contents.....	III
List of Figures .....	IV
List of Tables .....	V
Chapter -1-	
Introduction .....	1
Chapter -2-	
A- Experimental Set up .....	6
B- Mathematical expressions for cross section .....	19
C- Procedure .....	22
Chapter -3-	
Theoretical Aspects .....	26
Chapter -4-	
Experimental Data and Discussion .....	36
Appendix	
Computer Programs .....	45
References .....	53

LIST OF FIGURES

.....

Fig. 1- Beam Line Assembly .....	7
Fig. 2- Radiofrequency Ion Source .....	8
Fig. 3-A- Target System .....	10
3-(B-D)- Photographs of different views of the scattering chamber are shown in (3-B, 3-C and 3-D).....	12,13,14
Fig. 4- Pulse Counting Set.....	18
Fig. 5- Graph of ratio against pressure .....	24
Fig. 6- Electron detachment in "Complex Potential Model".....	27
Fig. 7- The behaviour of $f(t)$ as a function of $t$ .....	31
Fig. 8- The behaviour of $(t)$ as a function of $t$ .....	34
Fig. 9- Cross section for the production of Bromine atoms from negative ions in rare gases. The present measurements shown by dots with error bars, the continuous lines, Bydin and Dukel'skii (1957) experimental data.....	37
Fig. 10- Cross section for the production of Bromine positive ions from negative ions in rare gases. The present measurements shown by dots with error bars, the data of Lichtenberg et al. (1980), shown by circles.....	39
Fig. 11- Comparison between the Zero Range sudden approximation model of Gauyacq using the molecular energies of Olson and Liu, and the present measurements shown by dots....	43

.....

LIST OF TABLES

.....

Tab. 1- Types of the collision processes .....3

Tab. 2- Cross section for single electron detachment from  $\text{Br}^-$   
ions in a single collision with rare gas atom .....38

Tab. 3- Cross section for double electron detachment from  $\text{Br}^-$   
ions in a single collision with rare gas atom .....40

.....

## CHAPTER, 1

---

### INTRODUCTION.

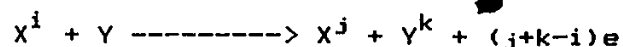
\*\*\*\*\*

The basic principle of determining the absolute collision cross sections of positive heavy ions in inert gases, experimentally and theoretically up to 1950 have been summarized and discussed by Massey and Burhop<sup>1</sup>.

In 1956 Dukelskii and Fedorenko<sup>2</sup> investigated the detaching processes for negative ions of the halogens and alkali metals, their measurements identified the double electron detachment from negative ions in a single collision process in the energy range from 5 to 17.5 keV. They found that the two electrons removal cross sections from halogen depend on energy. They pointed out that the magnitudes of the single electron detachment cross sections are big as compared with double electron detachment. In 1971 Matic and Cobic<sup>3</sup> found that the cross section of removal of two electrons always increases with the energy for carbon negative ions incident on rare gas target, for oxygen negative ions the cross section for single electron detachment increases with increasing target atomic number, but the inverse relationship was found between the cross section and the target atomic number in double electron detachment.

Since that time techniques have been refined such that now experimental cross sections are obtainable with smaller error. Present day experimental methods include projecting an energetic beam of ions or atoms through the atomic or molecular target and either determining the attenuation of the incident beam or measuring the growth rate and magnitude of the reaction products.

It is more convenient to simplify the interaction between an ion and a neutral atom by assuming  $(X^i)$  is the ionic particle of charge  $(ie)$  where  $(e)$  is the charge of single electron and the neutral particle is assumed to be  $(Y)$ . The interaction between the two partners can be represented by :



The cross section for this process denoted by  $(\sigma_{ij})$  where  $(i)$  represents the initial charge of the incident ions and  $(j)$  represents the final charge after the event. From the above equation when  $i=-1$  and  $j=k=0$  the process is single electron detachment whereas for  $i=-1$ ,  $j=+1$  and  $k=0$  the process is two electrons detachment.

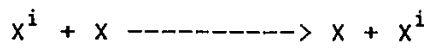
The energetic ion beam has been prepared and is moving in high vacuum towards the converter cell (collision chamber) which contain the gas targets.

Generally there are many processes which can occur within an inelastic collision between negative ions and neutral atoms. These processes are summarized in table -1- .

Table 1. Types of collision processes.

TYPES OF INTERACTION	PROCESSES
Single electron detachment	$X^- + Y \longrightarrow X + Y + e - \Delta E$
Double electron detachment	$X^- + Y \longrightarrow X^+ + Y + 2e - \Delta E$
Charge exchange	$X^- + Y \longrightarrow X + Y^- + \Delta E$

If both members taking part in the collision belong to the different species, then these type of collision processes are called "Asymmetric charge transfer", where  $\Delta E$  is equal to the electron affinity and/or ionization potential depending on whether the detachment process may happen in one or two steps. In the case when the ion beam and the gas target atoms are from the same species the process is called "Symmetric charge transfer", but for  $\Delta E=0$  the same process is called the "Resonant charge transfer", represented by:



Many experiments have been done to measure the absolute cross sections for the single and double electron detachment of halogens negative ions during their passage through the target gases in different energy ranges. In the low energy range the electron detachment cross section for halogens has been measured by Bydin and Dukelskii in 1957<sup>4</sup>. Lichtenberg, Bethge and Schmidt-Bocking in 1980<sup>5</sup> have measured the total electron detachment cross section for halogens in the energy range from 20 to 220 keV. Beside these measurements on halogens negative ions, many

other measurements have been done<sup>6,7,8,9</sup>. But still the theoretical interpretation is not so clear for electron detachment process from negative ions.

Theoretically the Zero Range potential theory<sup>10,11,12</sup> has been found suitable for predicting the electron detachment cross section for a negative ion in an atomic collision. The Zero-Range Potential Model is based on the assumption that the electron in the molecular state is weakly bound. The behaviour of this electron after the crossing point can be described by a wave function which satisfies the Schrodinger equation for a free particle. The interaction of the outer electron with the neutral diatomic molecule is approximated by a "Zero-Range Potential". The time dependence of this potential is responsible for the merging of the negative molecular ion with the continuous spectrum. There is another theoretical model, it gives a different interpretation for this process and is called the "complex potential model"<sup>12</sup>. This model is based on the assumption that the transition between the potential curves can only happen at the intersection point and for values of "R" which are less than " $R_{cr}$ ". The crossing point represents the start of break-up of the negative ion when it collides with the neutral atom and the merging of the negative ion states with the continuum spectrum. The interaction energy of the colliding particles in the complex potential model contains a real and an imaginary part. The width of the state after the crossing point is inversely proportional to the lifetime of the decaying state.

This thesis describes measurements of the absolute cross sections for the electron detachment process of bromine negative ions during their passage through the inert gas targets in the 10 to 100 keV energy range.

The single electron detachment cross section for the helium, argon and krypton targets shows some small energy dependence, while for neon its behaviour is energy independent, but for xenon, the heaviest gas target, it increases with the energy up to 30 keV and after that the oscillations start with values of cross sections about  $(0.95 \text{ to } 0.79 \cdot 10^{-15} \text{ cm}^2)$ .

The double electron detachment cross section generally shows some energy dependence in all gas targets.

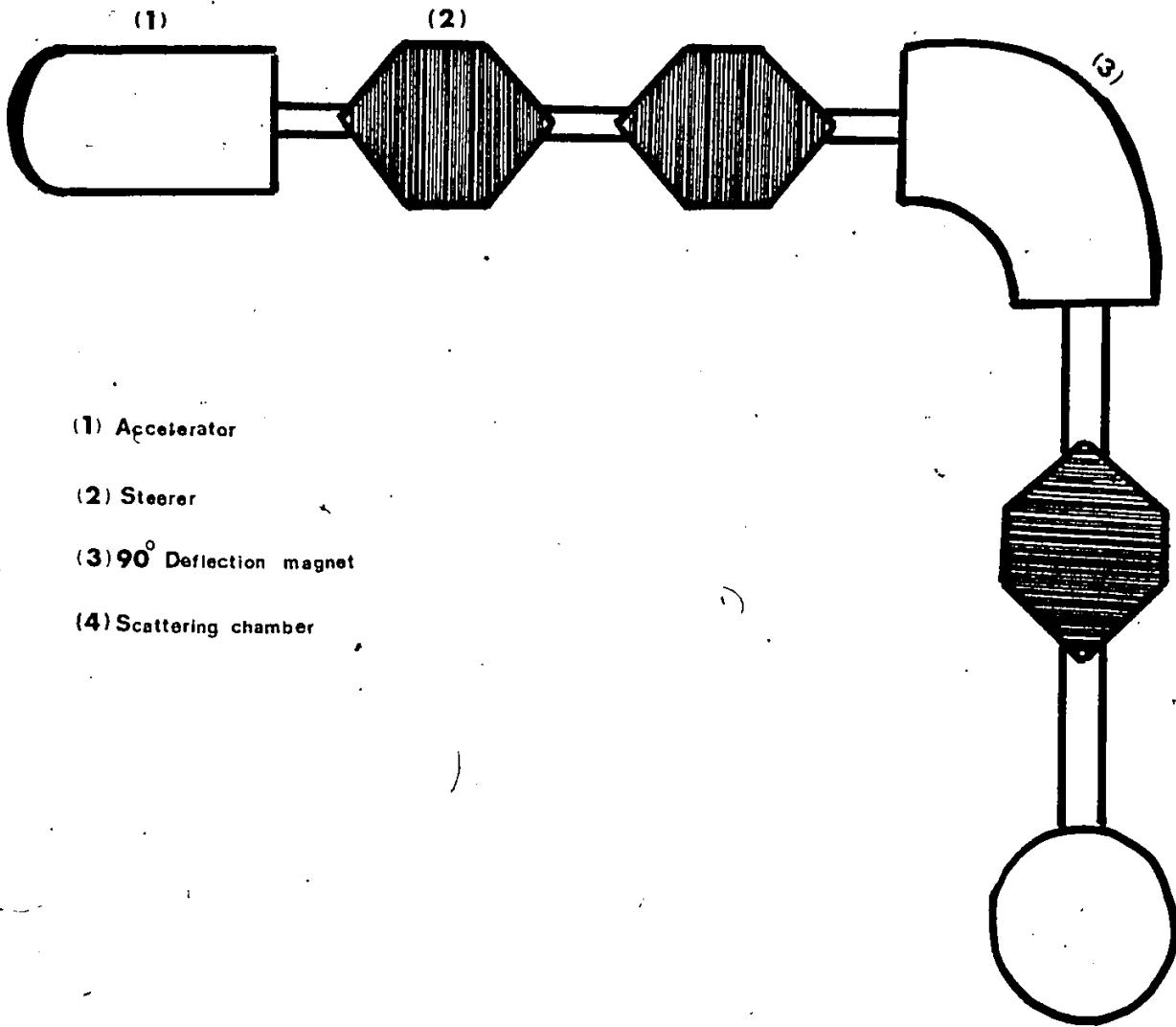
## CHAPTER 2

.....

### A- Experimental Set up \*\*\*\*\*:

The system for measuring electron detachment cross sections is schematically illustrated in fig (1). The type of ion beam and its energy could be accurately determined by the 150 KV accelerator (Model 150-1H, TEXAS NUCLEAR CORPORATION, AUSTIN, TEXAS.).

The bromine gas was ionized in a (25 M.Hz) radio-frequency ion source . The ion source essentially is a glass tube as is shown in fig (2). The basic idea of producing negative ions is to ionize the bromine gas inside the tube and the positive ions produced move towards the region of the canal where they were extracted. The negative ions are formed from the positive ions inside the canal by electron capture collisions with the residual gas. This type of ion source works very successfully for gases. The most convenient gas for the production of the  $\text{Br}^-$  ions beam is obtained by putting few drops of liquid "Br" in a separated glass tube provided with a tap to control the flow of the evaporated liquid to the ion source.



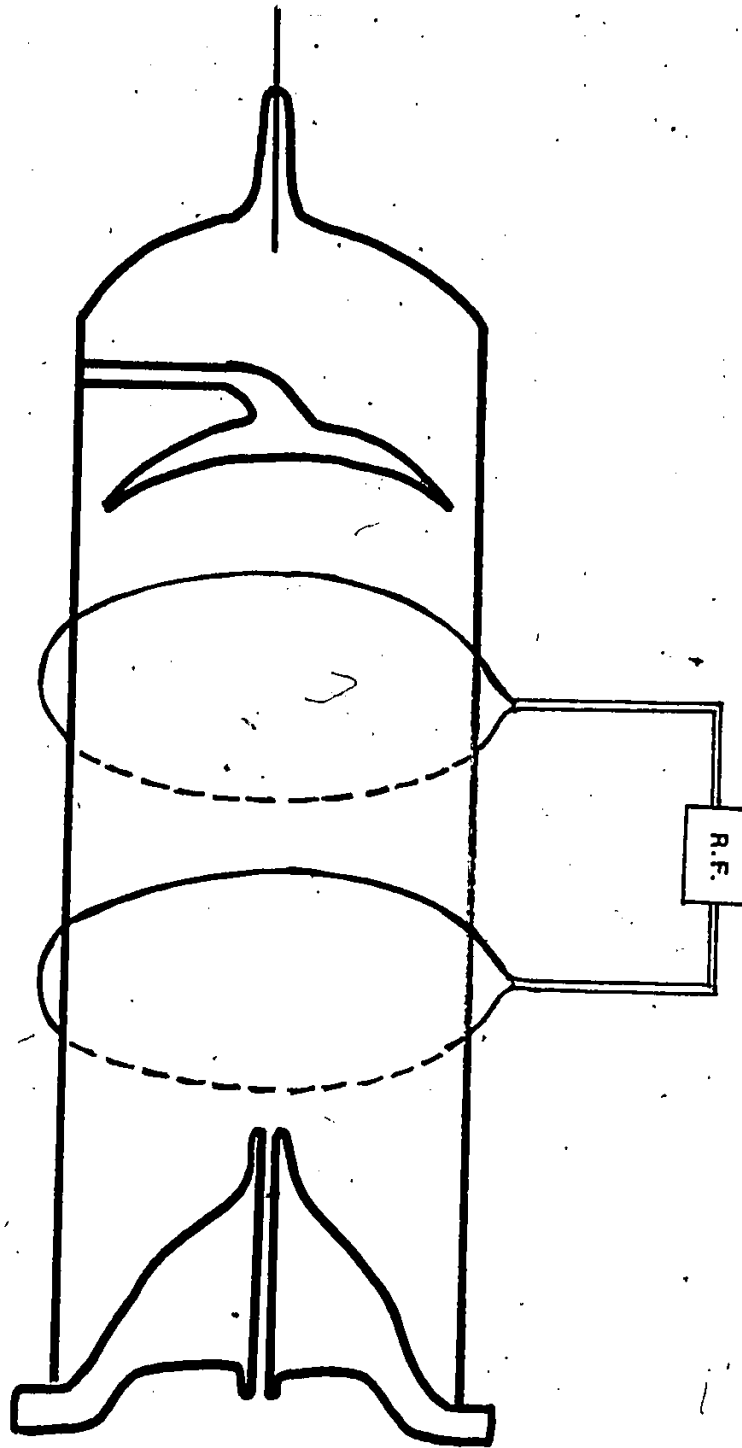
(1) Accelerator

(2) Steerer

(3) 90° Deflection magnet

(4) Scattering chamber

FIG\_1\_



Beam extractor

FIG. 2.

The length of the beam line is about 10 meters from the accelerator to the detectors. The whole beam line was maintained under pressure of about  $5 \times 10^{-7}$  Torr which is achieved by four diffusion pumps and one rotary pump. The diffusion pumps are placed at different places along the beam line and the vacuum is uniform along the beam line. The ion beam accelerated to the desired kinetic energy which are used in this work ranges from 10 to 100 keV. Three sets of steerers were used after the accelerator to make the projectile beam pass through the  $90^\circ$  magnet. This magnet deflected the beam through  $90^\circ$  and had a radius of 66 cm with uniform field and double focusing and has an energy resolution of about 0.1%. At about 4 meters from the accelerator there is an adjustable slit which is used to control the intensities of the ion beam. In the case of bromine this slit was kept wide open at low energies to keep the beam intensity large enough for the positive ions rate to be higher than the dark current on the channeltron.

The scattering chamber contains the target system which consists of the collimator, target gas cell, electrostatic deflector and the channeltrons as is shown in fig.3-A and 3-(B-D). The collimator and electrostatic deflector were located on a common base, the channeltrons were mounted on a separate plate mounted on the common base.

The collimator consisted of two slits "A" and "B", slit "A" of 0.5 mm and slit "B" of 0.45 mm diameter and 20 cm apart. Slit "B" is the entrance of the beam to the gas target cell of

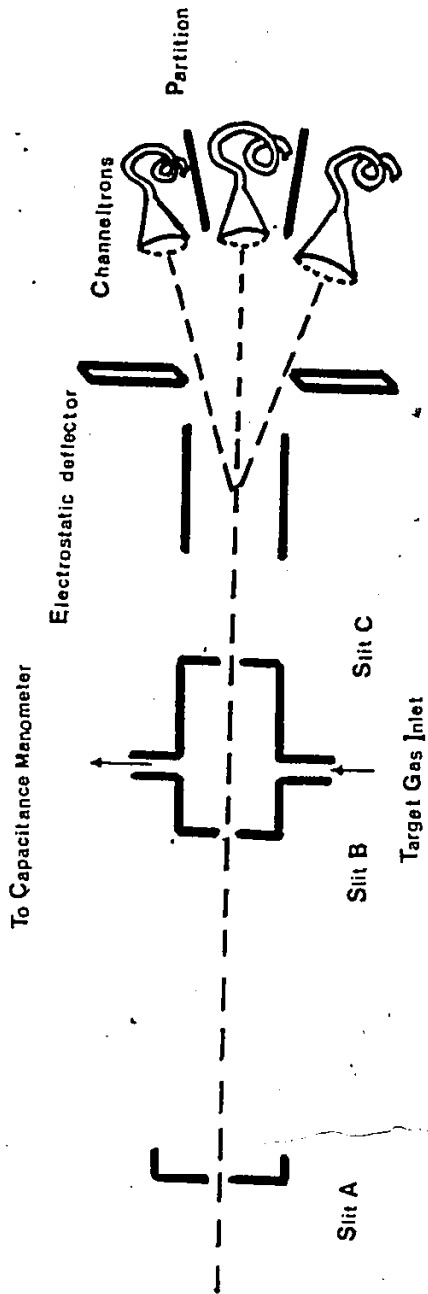


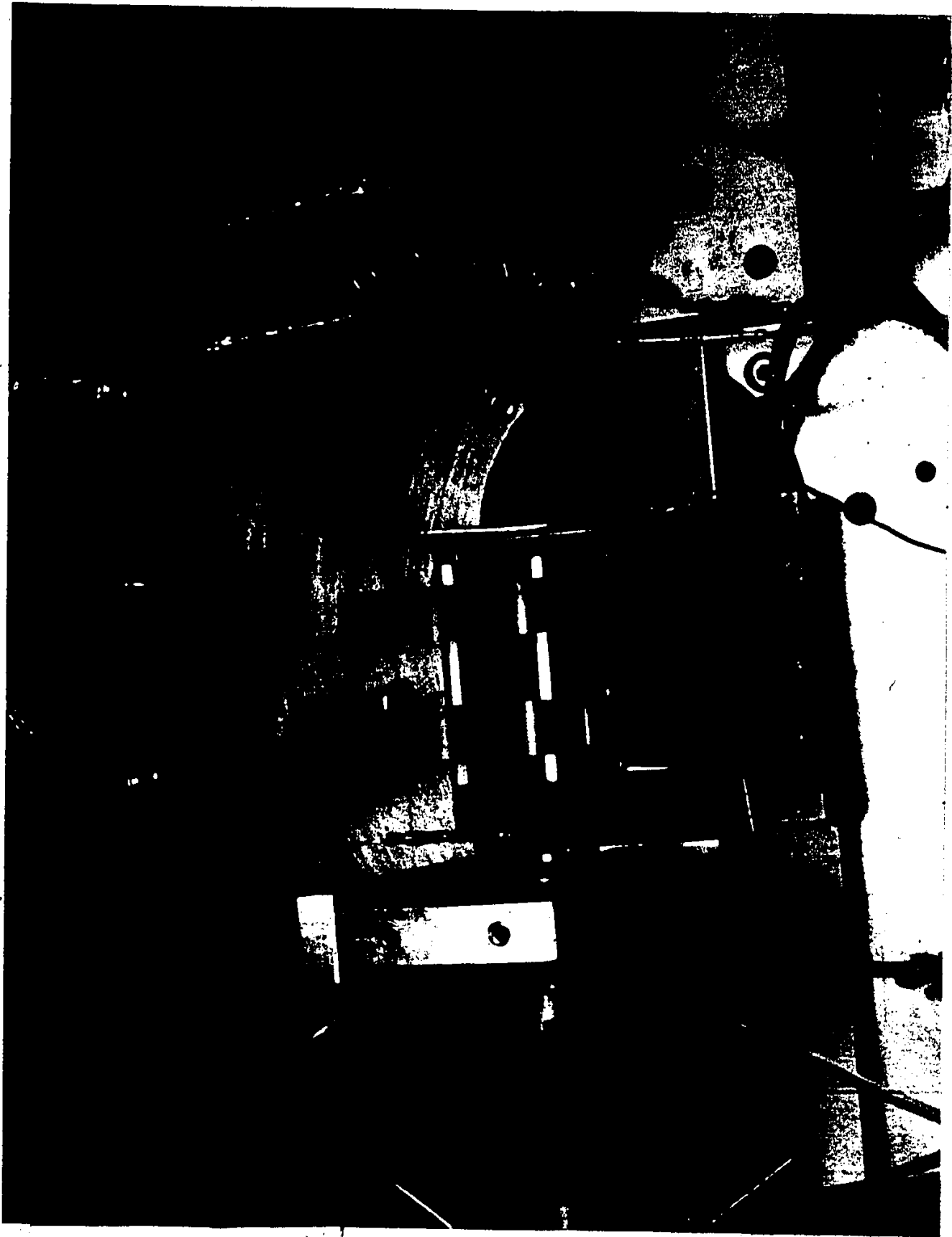
FIG. 3.A-

Fig. 3-(B-D)

.....

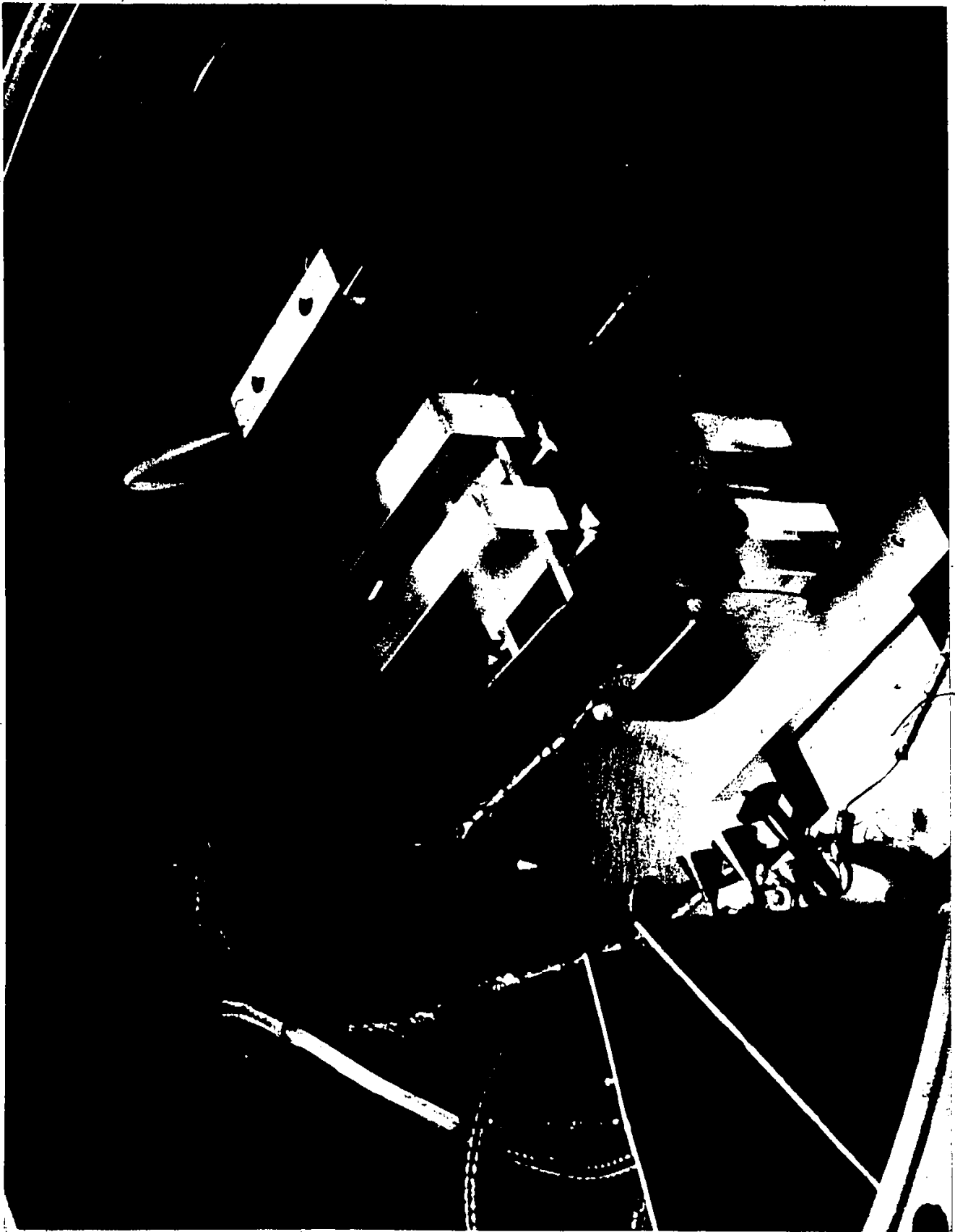
Photographs of different views of the Scattering Chamber, which consists of the target cell, electrostatic deflector and the channeltrons with the partitions.

.....



COLOURED PICTURES  
Images en couleur

FIG\_3.B\_



FIG\_3.C\_

COLOURED PICTURES  
Images en couleur



FIG\_3.D\_

COLOURED PICTURES  
Images en couleur

length 3.81 cm, this distance is assumed to be the effective length of the gas target in the electron detachment collision. The end of the gas target cell was defined by slit "C" which was made 1.5 mm diameter. The collimeter was mounted over two adjustable -V- blocks 10 cm apart, which helped in the alignment of the beam. The collimeter's geometry was set in such a way that no direct ions which did not pass through the collimeter could strike the target's exit aperture, because it was found that the misalignment of the beam could produce multiple scattering due to the edges of the apertures.

The pressure in the target cell was kept in the range between  $10^{-6}$  Torr to  $10^{-4}$  Torr. The flow of the target gas was controlled by a thermal mechanical leak. The target was kept thin enough to satisfy single collision conditions. The pressure inside the target was measured by two capacitance manometers (M.Ks-INSTRUMENTS, TYPE 145 BHS-1: 1 mmHg Head Baratron) to get accurate measurements with negligible drift on the pressure, the manometers were connected to the target chamber by suitable lengths of copper pipe.

The both gauges were found to be very sensitive to the variations of temperature, this was reduced by keeping the two gauges within a single wooden box. As a result of this treatment, the stability was much improved and the zero setting was quite good so that the drift was negligible. The calibration of these capacitance manometers were accurate enough so that the very small error could be neglected.

The electrostatic deflector was mounted on the common base at a distance of 1.7 cm, away from the slit "C", the electrostatic deflector consisted of two parallel plates with a separation of 1.9 cm, each plate has length of 5 cm. A grounded rectangular aluminum shield having a window of 1 cm width and 2.5 cm long was attached to the electrostatic plates facing the channeltrons. The main purpose for this was to prevent any electrons emitted from the electrostatic deflector to reach the channeltrons, because it was found in deflecting the particles at high energies that it needed big voltages across the electrodes and this could increase the probability of emitting electrons from the surface of the electrodes.

The counting system consisted of three channeltrons which were mounted side by side over a separate base which has three adjustable screws and two horizontal openings of width 1 cm and length 9 cm, to give the channeltrons free horizontal adjustment on the first one and the partitions on the second, these channeltrons were found to effect each other when the high voltage was applied across their tubes. To treat this two thin aluminum partitions of height 6 cm were mounted on the second opening behind the channeltrons in order to separate them and to prevent stray electrons passing from one to another. The channeltrons which are used for detecting the particles in this experiment were of two types. One was (B419 BL01 Phillips), the two others were of type (4039-C Galileo, Analytech Components Inc.). The pulse counting circuit which was connected to the

channeltrons is shown in fig. (4). The pulse signals which came from the channeltrons were fed into a pulse amplifier system, it consists of an emitter - follower - preamplifier, the pulse signal then was delivered further to the main amplifier which in turn delivered the amplified pulses to the discriminator and then to the scaler. For better channeltron stability, the applied voltages used on the channeltrons were kept within the recommended voltages. The counting rate was kept below 1k counts/sec<sup>14</sup>.

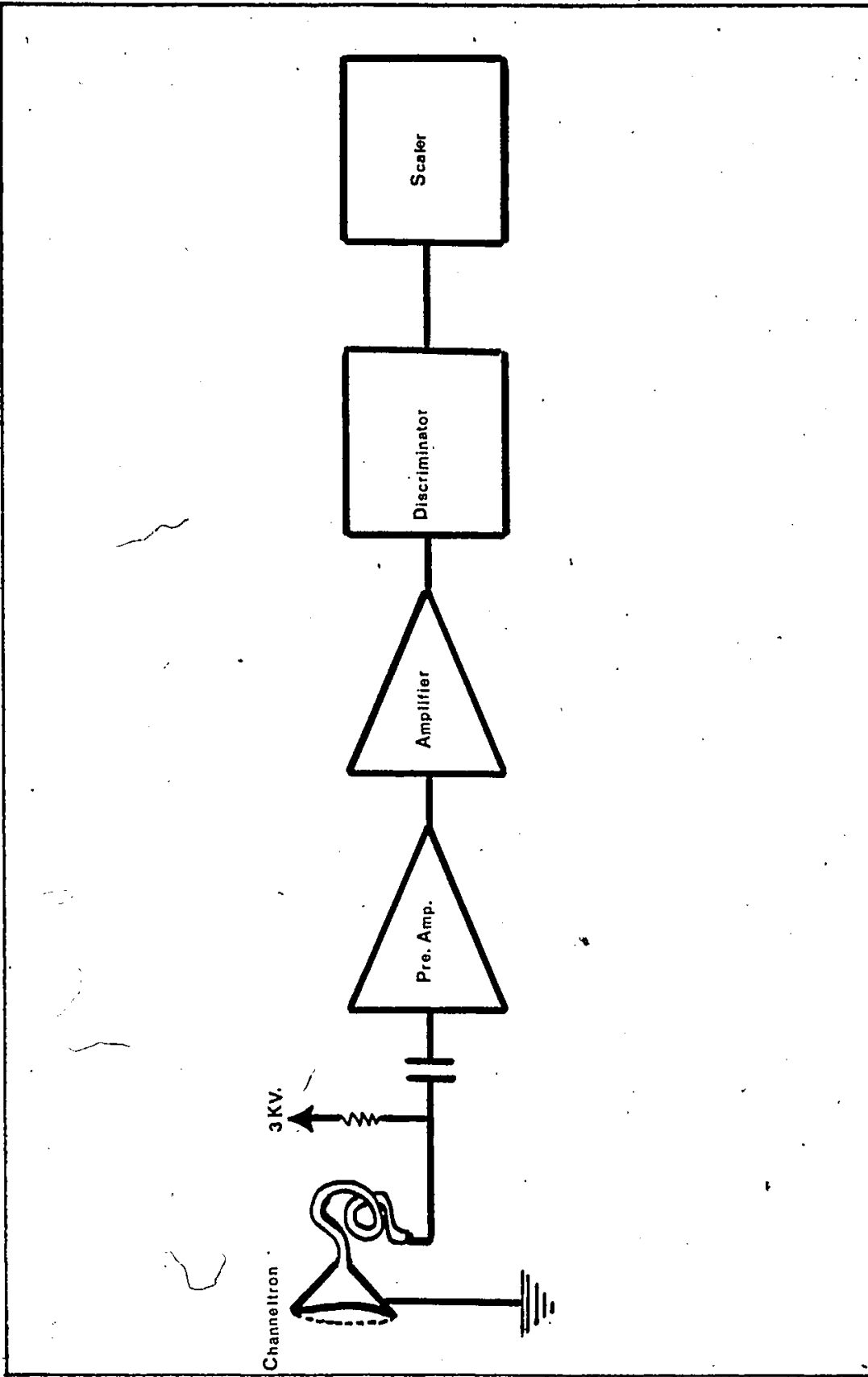


FIG -4-

**B-Mathematical expressions for cross section**  
 \*\*\*\*\*:

The detachment cross section for one electron or more can be described by ( $\sigma_{ij}$ ) which represents the probability of this process to occur, in the units of  $\text{cm}^2/\text{atom}$ , where (i) is the initial charge state of the incident ions and (j) is the final state of the ions after the collision.

The variation of charge state populations of an ion when it traverses through the gas target can be represented by<sup>15</sup> :

$$\frac{d\phi_i}{dt} = \sum_{j \neq i} \left[ \phi_j \sigma_{ji} - \phi_i \sigma_{ij} \right]$$

The above equation can be written in the form :

$$\frac{d\phi_i}{dt} = \sum_j \phi_j \sigma_{ji} \text{ ----- (1)}$$

Where  $\sigma_{ii} = - \sum_{j \neq i} \sigma_{ij}$  is substituted in the second term. In equation (1)  $\phi_i$  is the number of ions in charge state (i) before the collision and " $\phi_j$ " is the number of converted ions to the charge state (j) after their passage through the gas target of thickness (t), which represents the number of the gas target atoms per  $\text{cm}^2$ . It has to be measured as :

$$t = n X = A L P/R T$$

where (X) is the effective length of the target, (n) is the

number of target particles per unit volume, (p) is the target gas pressure in Torr, (L) is the path length in the target cell in cm, (A) is Avogadro's number, (R) is the gas constant and (T) is the absolute temperature of the gas .

Assuming the initial boundary condition is:

$$t = 0, \phi_i = \phi_{oi} \text{ and } \phi_{oj} = 0$$

The general solution for equation (1) becomes<sup>16</sup> :

$$\phi_j = \phi_{oi} \left[ \delta_{ij} + \sigma_{ij} t + \frac{t^2}{2} \sum_k \sigma_{ik} \sigma_{kj} + \frac{t^3}{6} \sum_{k,L} \sigma_{ik} \sigma_{kl} \sigma_{lj} \right] \text{----- (2)}$$

where " $\phi_{oi}$ " is the original ion beam intensity.

From equation (2) after simplification one can get :

$$\frac{\phi_j}{\phi_i} = \Phi = \frac{\sigma_{ij} t + \frac{t^2}{2} \sum_k \sigma_{ik} \sigma_{kj}}{1 + \sigma_{ii} t + \frac{t^2}{2} \sum_k \sigma_{ik} \sigma_{ki}}$$

where

$$\delta_{ij} = \begin{cases} 1 & \text{if } i=j \\ 0 & \text{if } i \neq j \end{cases}$$

The cross section can be written from above equation as :

$$\sigma_{ij} = \frac{\Phi}{t} \frac{(1 + \sigma_{ii} t + \frac{t^2}{2} \sum_k \sigma_{ik} \sigma_{ki})}{(1 + \frac{t}{2} \frac{\sum_k \sigma_{ik} \sigma_{kj}}{\sigma_{ij}})}$$

This expression for the cross section is in terms of the number of converted particles and the number of surviving particles which left without charge exchange. The other cross sections involved in this expression are obtained by neglecting the cross section for three and more electrons transfer, because they are very small.

By taking the first order of (t) and using the Binomial expansion one can get :

$$\sigma_{ij} = \frac{\Phi}{t} \left( 1 + \sigma_{ii} t \right) \left( 1 - \frac{t}{2} \frac{\sum_k \sigma_{ik} \sigma_{kj}}{\sigma_{ij}} \right)$$

$$\bar{\sigma}_{ij} = \frac{\Phi}{t} \left[ 1 + t \left( \bar{\sigma}_{ii} - \frac{\sum \bar{\sigma}_{ik} \bar{\sigma}_{kj}}{2 \bar{\sigma}_{ij}} \right) \right]$$

The expansion for :

$$\sum_k \bar{\sigma}_{ik} \bar{\sigma}_{kj} = \left( \sum_{\substack{k \neq i \\ j \neq i}} \bar{\sigma}_{ik} \bar{\sigma}_{kj} \right) + \bar{\sigma}_{ii} \bar{\sigma}_{ij} + \bar{\sigma}_{ij} \bar{\sigma}_{jj}$$

So,

$$\bar{\sigma}_{ij} = \frac{\Phi}{t} \left[ 1 + t \left( \bar{\sigma}_{ii} - \frac{\bar{\sigma}_{ii}}{2} - \frac{\bar{\sigma}_{jj}}{2} - \frac{\sum \bar{\sigma}_{ik} \bar{\sigma}_{kj}}{2 \bar{\sigma}_{ij}} \right) \right]$$

From the above equation one can get:

$$\begin{aligned} \bar{\sigma}_{ij} &= \frac{\Phi}{t} \left[ 1 + t \left( \frac{1}{2} \bar{\sigma}_{ii} - \frac{1}{2} \bar{\sigma}_{jj} - \frac{1}{2} \frac{\sum \bar{\sigma}_{ik} \bar{\sigma}_{kj}}{\bar{\sigma}_{ij}} \right) \right] \\ &= \frac{\Phi}{t} \left[ 1 + \frac{t}{2} \left\{ - \left( \sum_{k \neq i} \bar{\sigma}_{ik} + \bar{\sigma}_{ij} \right) + \left( \sum_{k \neq j} \bar{\sigma}_{jk} + \bar{\sigma}_{ji} \right) - \frac{\sum \bar{\sigma}_{ik} \bar{\sigma}_{kj}}{\bar{\sigma}_{ij}} \right\} \right] \end{aligned}$$

After simplification and rearrangement the different terms, we can get:

$$\bar{\sigma}_{ij} \left( 1 + \frac{\Phi}{2} \right) = \frac{\Phi}{t} \left[ 1 + \frac{t}{2} \left( \bar{\sigma}_{ji} + \sum_{\substack{k \neq i \\ k \neq j}} \left( \bar{\sigma}_{jk} - \bar{\sigma}_{ik} - \frac{\bar{\sigma}_{ik} \bar{\sigma}_{kj}}{\bar{\sigma}_{ij}} \right) \right) \right]$$

The final general expression for the cross section can be written

$$\bar{\sigma}_{ij} = \left( \frac{\Phi}{1 + \Phi/2} \right) \frac{1}{t} \left[ 1 + \frac{t}{2} \left( \bar{\sigma}_{ji} + \sum_{\substack{k \neq i \\ k \neq j}} \left( \bar{\sigma}_{jk} - \bar{\sigma}_{ik} - \frac{\bar{\sigma}_{ik} \bar{\sigma}_{kj}}{\bar{\sigma}_{ij}} \right) \right) \right] \text{----- (3)}$$

The particular approximations which are used in this derivation depend on the situation of the experiment for a particular process and on the measurements which are available for the cross sections in the final expression.

C- PROCEDURE  
\*\*\*\*\*:

The bromine negative ions beam was formed and travels through three sets of magnetic steerers and "90°" deflecting magnet which has the ability to select the desired particles, and is good enough to separate various isotopes.

To identify the selected particles, a mass spectrum was made at each energy before the experiment.

The gas target was kept in equilibrium all the time, thin enough to maintain single collision conditions in target cell, during the experiment.

After the collisions the final products of the initial beam emerged out of the target cell via slit "C".

The beam was then passed through the parallel electrostatic deflector plates, by putting suitable voltages across it's plates, the ions are separated from the rest of the neutral particles which left after the collisions. The deflected components are detected simultaneously by two channeltrons which were mounted at the deflected position, the neutral particles which remain in the same direction are detected by the third channeltron which was mounted at the straight through position. These particles produced pulses in the channeltron electron

multiplier (CEM) which were amplified and counted on three scalars. The electrical circuit of the (CEM) and pulse counting system, are shown in fig (4).

At each energy several measurements were made by changing the voltages on the thermal-mechanical leak which controls the pressure of the target gas. The pressure in the target was left for a some time until it has become stable.

After collecting the data a rough estimation of the cross sections were made by plotting a graph of the ratio " $\phi^0 / \phi^-$ " for single electron detachment and " $\phi^+ / \phi^-$ " for double electron detachment as the Y-axis against the pressure of the gas target as the X-axis.

The rough cross section was calculated by the formula :

$$\sigma_{ij} = \frac{1.0351 \times 10^{-19} \times T \times \text{slope}}{L}$$

Where (L) is the effective length which is 3.81 cm, (T) is the absolute temperature. A typical graph of the ratio against the pressure is shown in fig (5).

In the graph the straight line passed through the experimental points does not start from the origin but starts from a small positive value of the ratio at zero pressure. This is due to the fact that the negative ions beam made some collisions with the residual gas before the target cell. But the determination of the cross section depends mainly on the slope of the line and not on the intercept point.

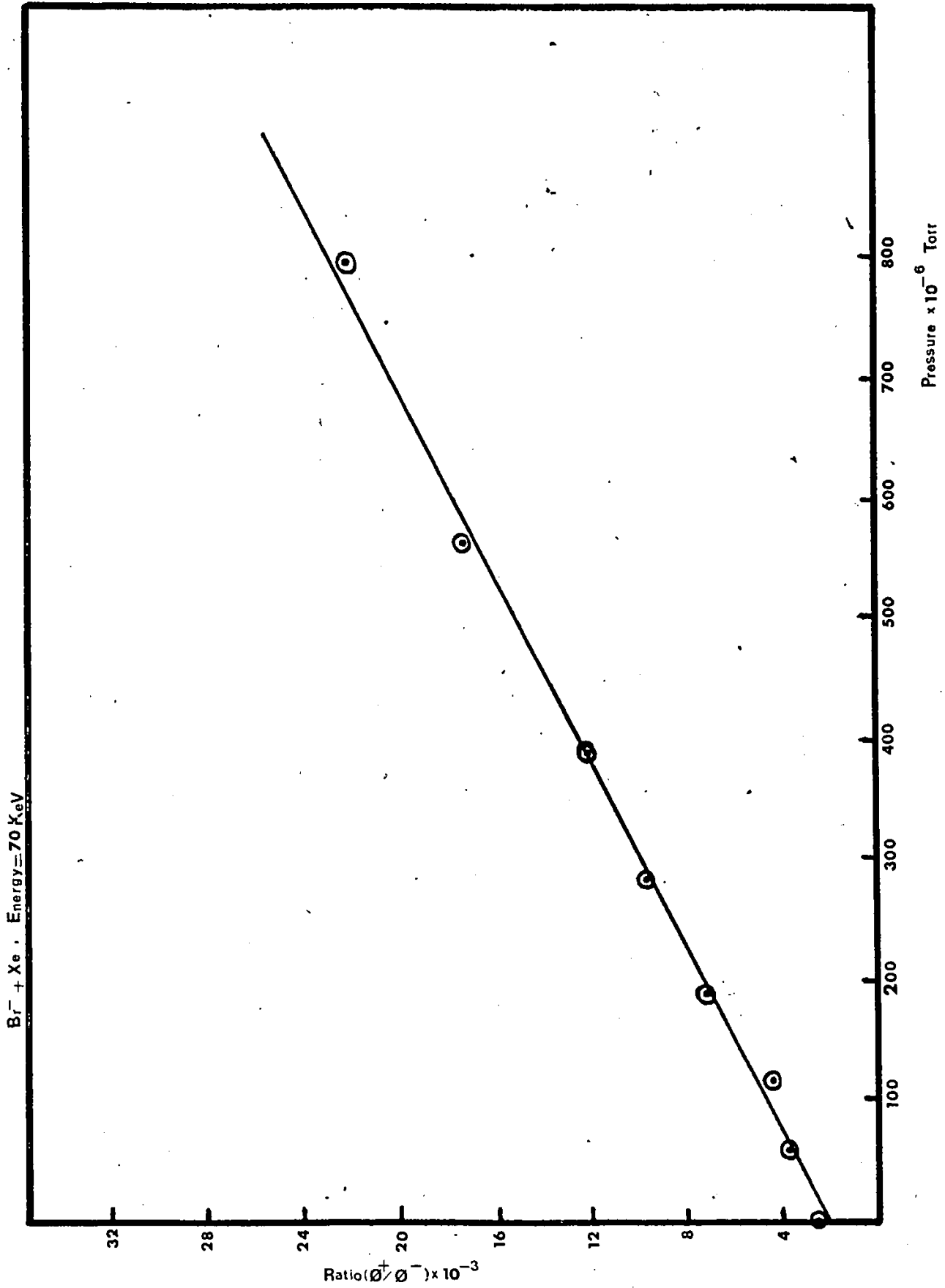


FIG -5-

For high numerical reliability in determining the cross sections and to calculate the experimental statistical errors, computer programmes were designed which were used for single and double electron detachment by making a least square fit to the equation (3) of the general cross section formula.

## CHAPTER 3

.....

### THEORETICAL ASPECTS

\*\*\*\*\*

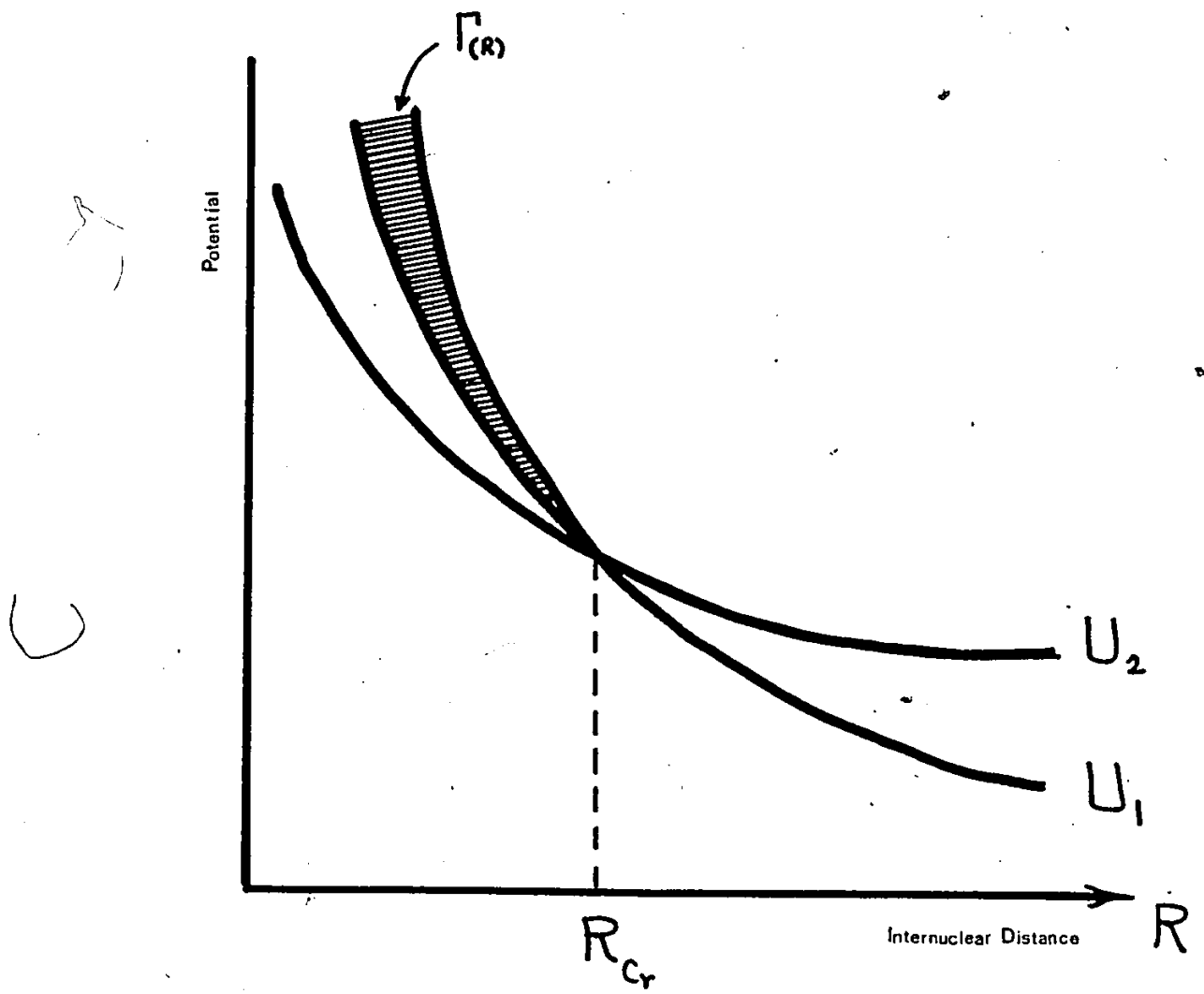
#### " COMPLEX POTENTIAL "

\*\*\*\*\*:

This model proposes that when a moving particle " $X^-$ " approaches a particle "Y" they form potential energy curves, the extra electron can be detached by making a transition from a bound to an unbound state through the crossing point as it shown in fig (6).

At large values of the internuclear distance "R" the potential energy curve " $U_2$ " of the system  $(X+Y+e)$  lies above the potential energy curve " $U_1$ " of the system  $(X^-+Y)$  by an amount equal to the electron binding energy or in other words equal to the electron affinity of the atom X .

The transition from the system " $U_1$ " to the system " $U_2$ " can only occur by breakup of the negative ion when it collides with the atom and this occurs at the crossing point " $R_{cr}$ " and at any distance where the closest approach  $R_{min} < R_{cr}$  .



FIG\_6\_

For large value of the distance "R" the negative molecular ion  $(XY)^-$  is in a bound state, but as the separation between the nuclei becomes less than the crossing point " $R_{cr}$ " in which the potential energy curves reaches the continuum, the bound state merges with the continuum. Therefore describing the energy of the negative ion state after the crossing point as<sup>13</sup> :

$$W(R) = V(R) - \frac{1}{2}i\Gamma(R).$$

The width of the complex portion ( $\Gamma(R)$ ) is inversely proportional to the lifetime of the state at ( $R < R_{cr}$ ). In absence of detachment ( $\Gamma(R)$ ) equal to zero and the potential represent the real part only which determine the elastic scattering cross section. The expression for the total electron detachment cross section is obtained from<sup>17</sup> :

$$\sigma_{Det.} = \int_0^{R_{cr}} 2\pi [1 - P_s(\rho)] \rho d\rho$$

where  $P_{Det.} = 1 - P_s(\rho)$

and  $\rho = R_{cr} \left[ 1 - \frac{U(R_{cr})}{E} \right]^{1/2}$

E is the kinetic energy of the particles in c.m. system, is related to the laboratory energy by:

$$E = \frac{M_2 E_{lab.}}{M_1 + M_2}$$

where  $M_1$  is the mass of the beam particle and  $M_2$  is the mass of the target particle, " $U_{(R_{cr})}$ " is the potential energy which is representing the interaction between the negative ion and the atom at the crossing point " $R_{cr}$ ", and " $\rho$ " is the impact parameter.

" ZERO-RANGE POTENTIAL "  
\*\*\*\*\*:

The zero-range potential was proposed in 1964 by Demkov, to find the suitable explanation for electron detachment in negative ion - atom collisions.

His treatment started by assuming that the transition of the electron from the energy state of the negative molecule occurs when it comes very close to the boundary of the continuous spectrum. The bound state of the negative molecular ion decays when "R" become smaller than " $R_{cr}$ " ( the crossing point ) with the formation of a wave packet from the states of continuous spectrum containing the wave function of the outer electron. For "R" greater than " $R_{cr}$ " the discrete energy level exists.

The electron which is detached from the negative molecule when the event occurs was already loosely bound due to the near approaching of a negative ion " $X^-$ " towards an atom "Y" in this case the outer electron is far enough from the neutral

diatomic molecule core, so that one can consider the electron in that part of the space is free with a wave function satisfying the Schrodinger equation for free particles. This wave packet has dimensions much larger than the region of the effective potential.

The interaction between the outer electron and the neutral molecule core is approximated by a zero-range potential.

The wave function for the outer electron assumed to be spherically symmetric, varies with the time as shown by the equation :

$$\left( -\frac{1}{2} \frac{\partial^2}{\partial r^2} - i \frac{\partial}{\partial t} \right) \Psi(r,t) = 0 \text{ ----- (1)}$$

With the boundary condition :

$$\frac{1}{\Psi} \frac{\partial \Psi}{\partial r} \Big|_{r=0} = f(t) \text{ ----- (2)}$$

The behaviour of the function " f(t) " with in the time interval extended from (-∞ to +∞) is displayed in the figure ( 7 ).

The behaviour of " f(t) " with respect to the reaction can be divided as follows. In region "I" and "III" which corresponds to "t < t<sub>1</sub>" and "t > t<sub>2</sub>" respectively, the function "f(t)" is negative and the discrete energy level exists as a bound state. For "f(t)=0" the merging of the discrete energy level take place with the continuous spectrum and in region "II" for "t<sub>1</sub> < t < t<sub>2</sub>" the function "f(t)" is positive and the bound state decay within the continuum.

Demkov calculated the survival probability at " R<sub>min</sub> << R<sub>cr</sub> " by using linear approximation<sup>10</sup> :

$$f(t) = \beta t$$

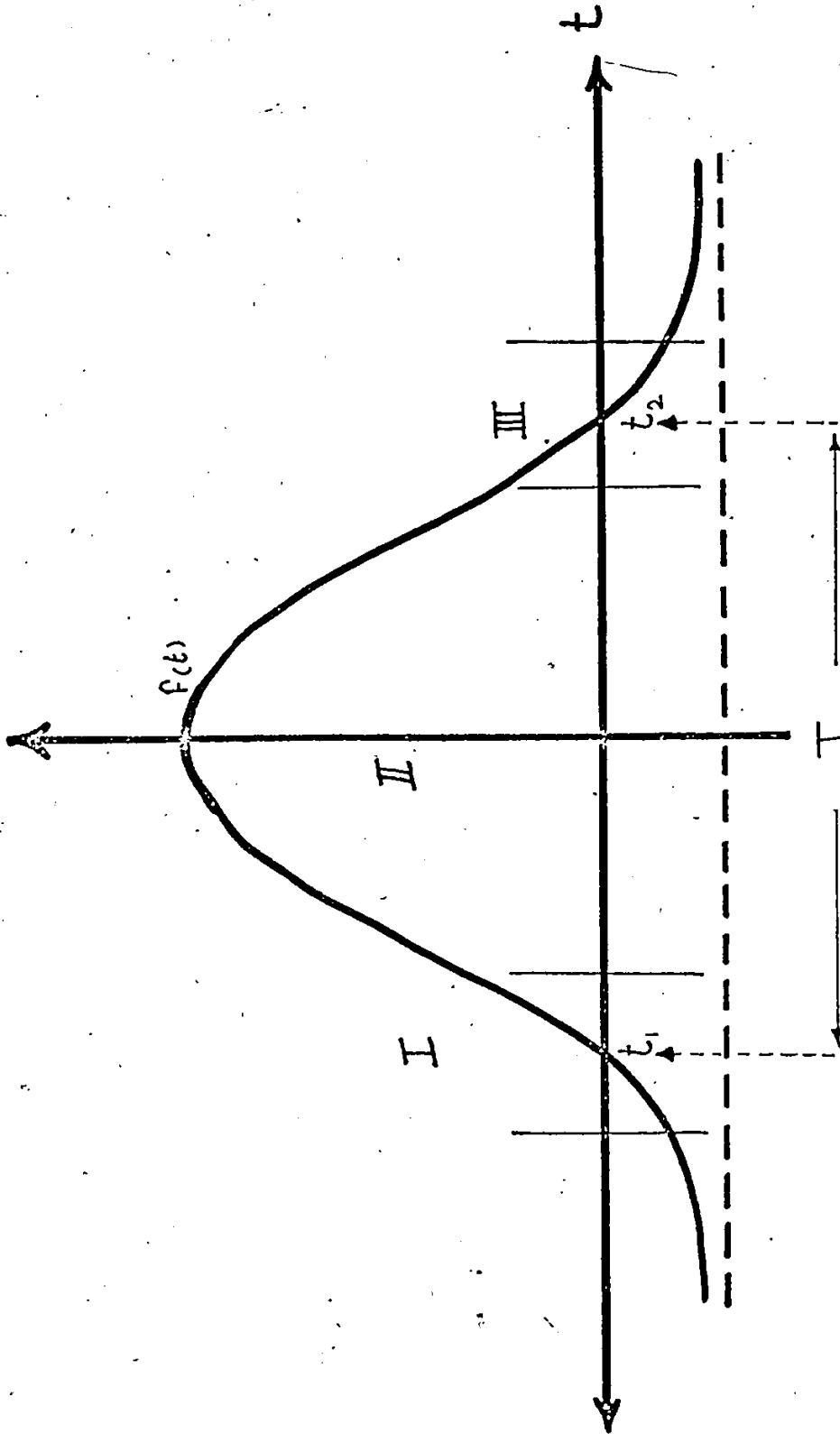


FIG -7- 7

Where " $R_{\min}$ " is the distance of closest approach and " $\beta$ " is adjustable parameter, ultimately he obtained .

$$P_s = \frac{2\pi}{\beta^2 T^3} \text{ ----- (3)}$$

Where "T" is the collision time and " $P_s$ " is the survival probability. Demkov's model was unable to give the correct expression for electron detachment probability at " $R_{\min} \approx R_{cr}$ ". The difficulty was solved by Devdariani who used a more general approximation than Demkov's approximation, it is given by<sup>11</sup> :

$$F(t) = -\alpha t^2 + \beta$$

Where " $\alpha$ " and " $\beta$ " are adjustable parameters, and has a big effect on the detachment probability " $P_d$ " due to value of " $\lambda$ " which is given by :

$$\lambda = \beta / \alpha^{1/5}$$

Where  $\alpha = \dot{F}(t) / 2t_1$  ,  $\beta = -t_1 \dot{F}(t) / 2$  and

" $t_1$ " is the time at the crossing point when the bound state and the continuous spectrum intersect each other.

The equation for " $P_d$ " is given by :

$$P_d = 0.62 + 0.42\lambda + 0\lambda^2 \text{ ----- (4)}$$

After Devdariani, Gauyacq<sup>12</sup> has pointed out that Demkov's<sup>10</sup> and Devdariani's<sup>11</sup> approximations do not give good agreement for  $H^- + He$  collision system, so that he solved the problem by using sudden approximation.

The behavior of the system can be explained by dividing it into two limits of time as shown in fig (8).

First for large time (when  $t \rightarrow \infty$ ) the wave function of the system develop adiabatically with the time and no transitions occur. The second region of the time which is between " $\pm t_1$ " represents the region of validity of the sudden approximation in which he replaced the smoothly continuous varying function " $f(t)$ " by a step function at the time ( $\pm t_1/2$ ), in this region the particles become very close to each other during the collision and the binding energy of the outer electron is sufficiently weak. The limit of time between " $\pm t_1$ " one can obtain by equating the inverse of the characteristic time of variation " $T_V$ " with the inverse of the characteristic time of the bound state " $T_C$ " as<sup>12</sup> :

$$\left( \frac{1}{\epsilon} \frac{d\epsilon}{dt} \right)_{t=t_1} = \epsilon(t_1) \text{ --- (5)}$$

Where  $(T_V)^{-1} = \frac{1}{\epsilon} \frac{d\epsilon}{dt}$  ,  $(T_C)^{-1} = \epsilon$  and " $\epsilon$ " is

the binding energy of the outer electron.

By changing the time variable to the internuclear separation "R" he got:

$$\frac{1}{\epsilon(R)} \frac{d\epsilon}{dR} v \left( 1 - \frac{V(R)}{E} - \frac{b_c^2}{R^2} \right)^{1/2} = \epsilon(R)$$

Where " $V(R)$ " is the potential energy, " $b_c$ " is the impact parameter and " $v$ " is the velocity of the particle.

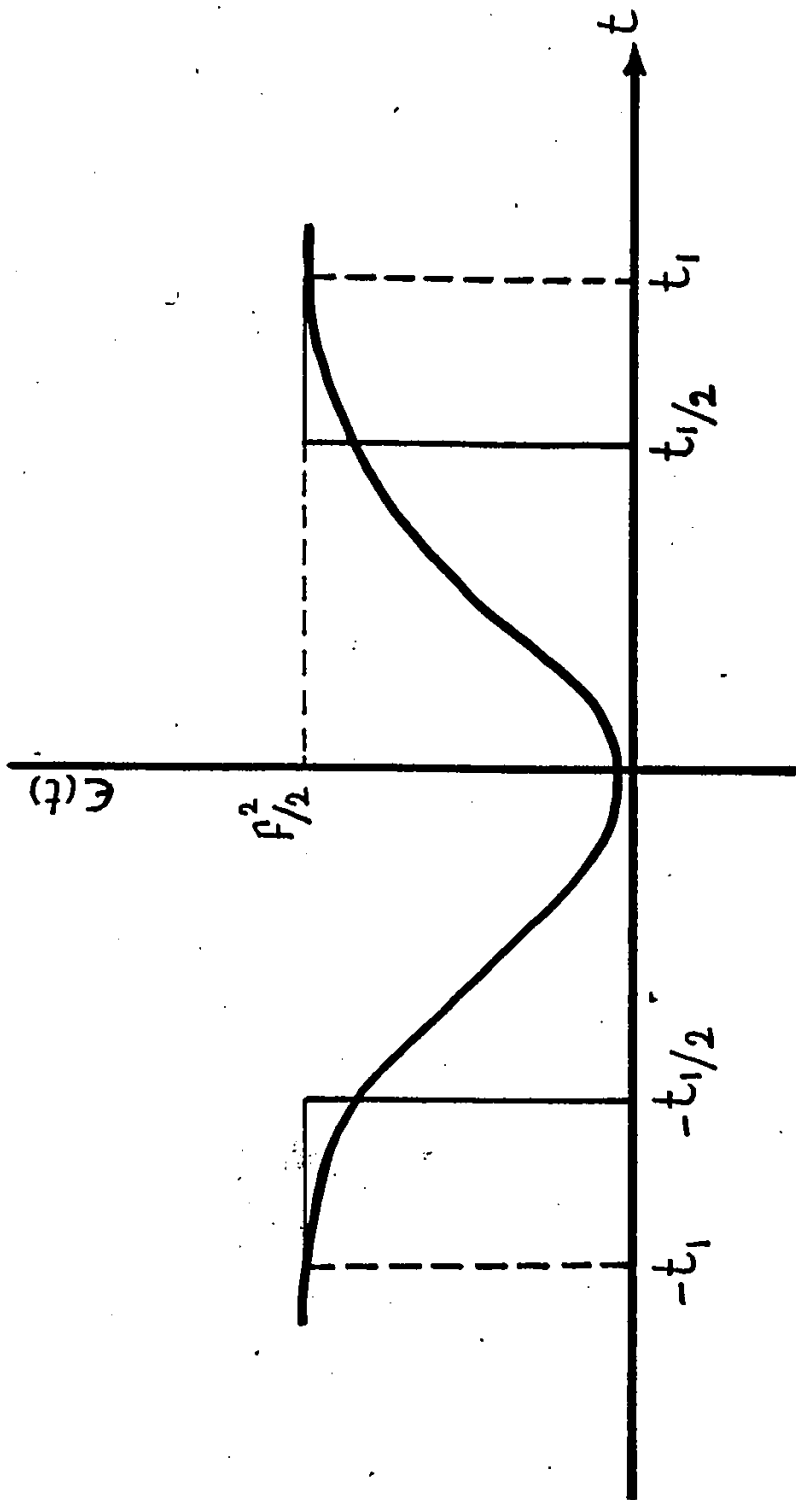


FIG -8-

The solution for this equation at the limit of adiabatic behavior at time "t<sub>1</sub>", as obtained by Gauyacq is given by :

$$t_1 = (R_M - R_C) / 4v \left( 1 - \frac{V(R_M)}{E} - \frac{b_c^2}{R_M^2} \right)^{1/2}$$

Where "R<sub>M</sub>" is the limit of the adiabatic behavior.

Within the sudden approximation region the impact parameter "b" plays an important role for the detachment cross section from the negative ions as "b" increases the time which the system spends in the active region decreases, so that the spread of the wave packet decreases. It was found that the threshold impact parameter "b<sub>th</sub>" is independent of the time which is spent by the particle in the active region. Due to this reason the appearance of the threshold in the detachment process is not effected by the time, therefore the expression for the detachment cross section can be given as<sup>12</sup> :

$$\begin{aligned} \sigma_{Det.} &= \pi b_{th}^2 \cdot P_S = 0.73 \pi b_{th}^2 \\ &= \pi R_C^2 \left( 0.73 + \frac{0.73 \times 8^{2/5}}{3.35} \frac{\alpha^{1/5}}{\beta_0} \right) \dots \dots (6) \end{aligned}$$

Where  $b_{th} = R_C \left( 1 + \frac{8^{2/5}}{3.35} \frac{\alpha^{1/5}}{\beta_0} \right)^{1/2}$ .

## CHAPTER 4

.....

### " EXPERIMENTAL DATA AND DISCUSSION "

\*\*\*\*\*

In the present study, the single and double electron detachment cross sections " $\sigma_0$ " and " $\sigma_{-1}$ " for  $\text{Br}^-$  ions on the rare gas targets in the ion energy from 10 keV to 100 keV were measured. The " $\sigma_0$ " cross sections are plotted on a logarithmic energy scale in fig. (9) and are presented in table (2), while the " $\sigma_{-1}$ " cross sections are plotted against the ion energy on a linear scale in fig. (10) and are presented in table (3).

The error bars shown on every point are obtained from the least square fit. In these figures the data which was obtained from other investigations is also shown where it exists.

For " $\sigma_0$ " in the collision between  $\text{Br}^-$  with the rare gases, the fig. (9) shows the points which were obtained by Bydin

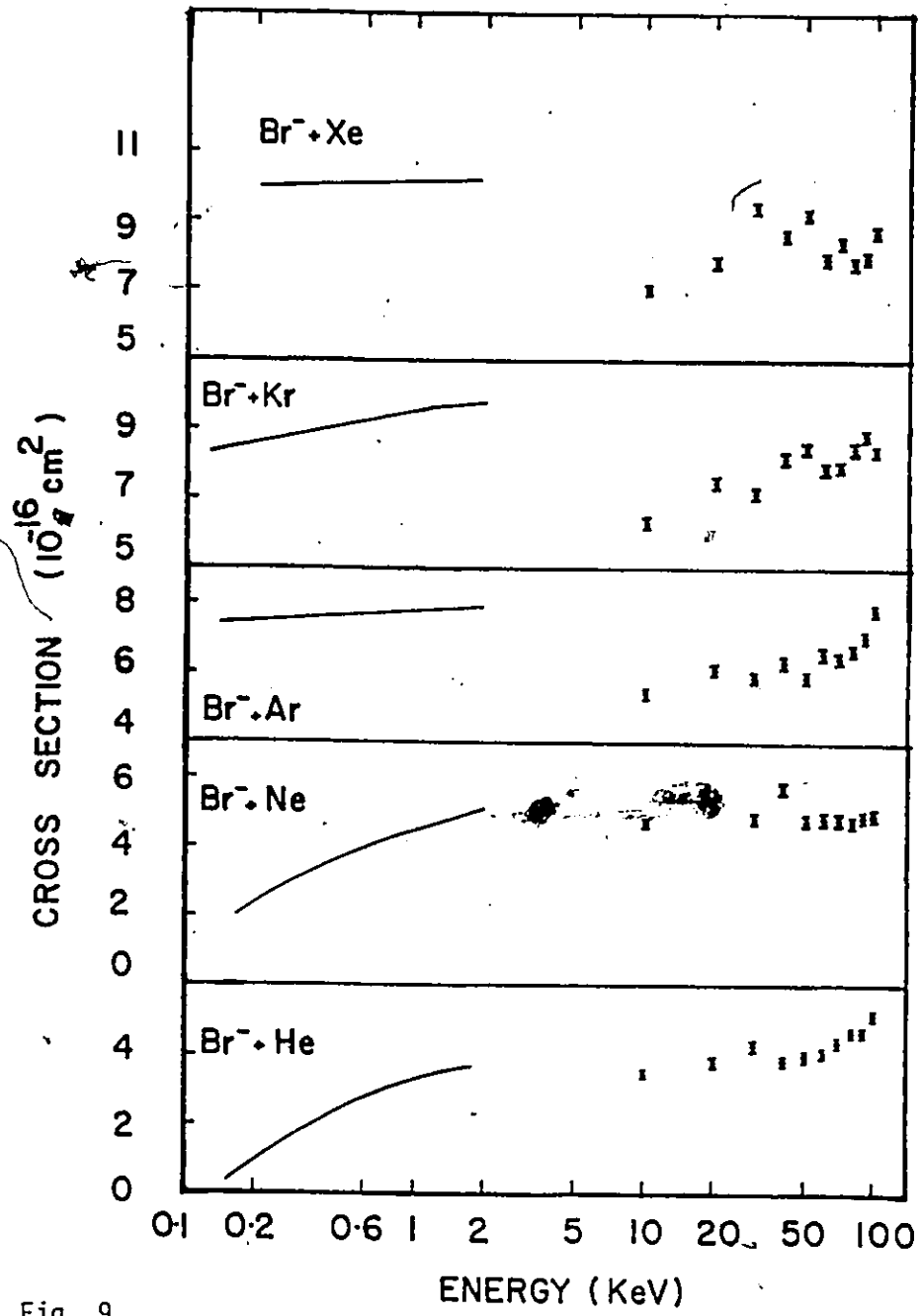


Fig. 9  
 -----: Cross section for the production of Bromine atoms from negative ions in rare gases. The present measurements shown by dots with error bars, the continuous lines, Bydin and Dukel'skii (1957) experimental data.

Table 2. The cross section for single electron detachment from  $\text{Br}^-$  in a single collisions with rare gas atoms.

Incident ion beam energy ( KeV )	( CROSS SECTIONS )				
	$\text{Br}^- \rightarrow \text{He}$ ( $10^{-15}$ )	$\text{Br}^- \rightarrow \text{Ne}$ ( $10^{-15}$ )	$\text{Br}^- \rightarrow \text{Ar}$ ( $10^{-15}$ )	$\text{Br}^- \rightarrow \text{Kr}$ ( $10^{-15}$ )	$\text{Br}^- \rightarrow \text{Xe}$ ( $10^{-15}$ )
10	0.35	0.47	0.54	0.64	0.71
20	0.39	0.53	0.62	0.76	0.78
30	0.43	0.49	0.59	0.72	0.95
40	0.39	0.57	0.63	0.82	0.87
50	0.40	0.48	0.59	0.85	0.93
60	0.42	0.49	0.66	0.80	0.80
70	0.44	0.48	0.65	0.80	0.84
80	0.47	0.47	0.67	0.85	0.78
90	0.48	0.49	0.71	0.89	0.80
100	0.52	0.49	0.78	0.85	0.87

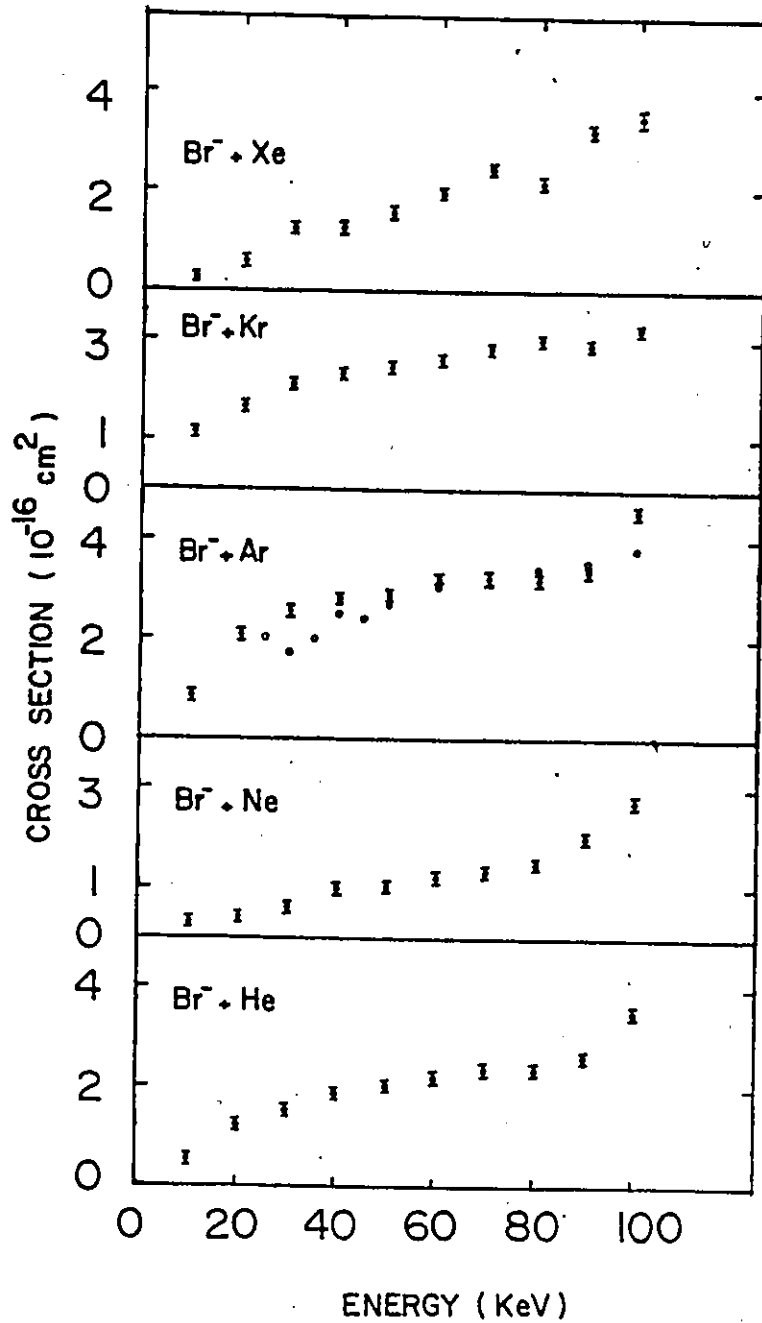


Fig. 10: Cross section for the production of Bromine positive ions from negative ions in rare gases, the present measurements shown by dots with error bars, the data of Lichtenberg et al. (1980), shown by circles.

Table 3. The cross section for double electron detachment from  $\text{Br}^-$  in a single collisions with rare gas atoms.

Incident ion	( CROSS SECTIONS )				
beam energy ( KeV )	$\text{Br}^- \rightarrow \text{He}$ ( $10^{-16}$ )	$\text{Br}^- \rightarrow \text{Ne}$ ( $10^{-16}$ )	$\text{Br}^- \rightarrow \text{Ar}$ ( $10^{-16}$ )	$\text{Br}^- \rightarrow \text{Kr}$ ( $10^{-16}$ )	$\text{Br}^- \rightarrow \text{Xe}$ ( $10^{-16}$ )
10	0.52	0.31	0.85	1.13	0.24
20	1.23	0.41	2.07	1.67	0.57
30	1.55	0.61	2.54	2.13	1.26
40	1.90	1.00	2.81	2.33	1.27
50	2.04	1.06	2.88	2.46	1.57
60	2.24	1.23	3.22	2.63	1.98
70	2.39	1.33	3.22	2.87	2.44
80	2.39	1.53	3.21	3.05	2.18
90	2.62	2.03	3.36	2.90	3.22
100	3.54	2.75	4.59	3.25	3.48

and Dukel'skii at low energy. Their points provide a good extrapolation to our points in  $\text{Br}^-$  ions colliding with the (He) and (Ne) gas targets assuming the prediction for the behavior of the cross sections within the energy gap between their energy range and our energy range are extend linearly with our points. In other words above about 2 keV the general behavior of the cross section becomes energy independent. There is some indication in the He gas target at 60 keV to 100 keV of some excitation behavior took place as a result of the collision. But for other gas targets Ar, Kr and Xe the extrapolation of their data does not give good agreement. One can say that the (Ar) and (Kr) the cross sections roughly increase with energy. The points show some oscillation. With the (Xe) target the situation shows an increase up to 30 keV and after that the oscillations start with values of cross sections about (0.95 to  $0.79 \cdot 10^{-15} \text{ cm}^2$ ).

The cross section for single electron detachment shows strong target mass dependence as shown in fig. (9), this behaviour is also observed in other halogen<sup>6,8</sup> negative ion collisions with the rare gases, with the exception of the (Ne) gas target where " $\sigma_0$ " is smaller than (He) gas target.

The defect in the complex potential model from an theoretical and experimental point of view is that it is restricted by the assumption that the electron detachment could occur at the crossing point " $R_{cr}$ " and in the complex region where " $R < R_{cr}$ ", so that the detachment probability at "R" less than " $R_{cr}$ " is

equal to unity, but is equal to zero for any "R" greater than " $R_{cr}$ ". Besides, the theory neglects some kind of tunnelling effect with some probability of detachment before the crossing radius " $R_{cr}$ " is reached.

The experimental data for ( $Br^-$ ) ions colliding with the (He) gas target has been compared with the Gauyacq's zero - range as shown in fig. (12) by using the potential energy curve which is calculated by R.E.Olson and B.Liu<sup>18</sup>. Our data shows good agreement in energy range restricted between 20 keV to 70 keV, the experimental cross section for an energy above 70 keV shows a rise with energy, probably due to some excited states of both negative ions and the neutral particles which are not included in the zero-range model.

The cross section for double electron detachment shows a rough energy dependence with the rare gas target, as shown in fig. (10).

The data which is taken from the work of Lichtenberg, Bethge and Schmidt-Bocking where they measured the " $\sigma_{Total}$ " and " $\sigma_{-}$ " cross sections for  $Br^-$  ions with (Ar) gas target in the energy range extending from 20 keV to 220 keV provide a very good and close agreement to our data.

It was found<sup>7,8,9</sup> that " $\sigma_{-}$ " has an unusual behavior for  $F^-$  ions and  $Cl^-$  ions in their collision with the rare gases, this behavior shows a larger magnitude in light targets than for the heavier targets.

This behavior was related to the ionic beam and target ionization

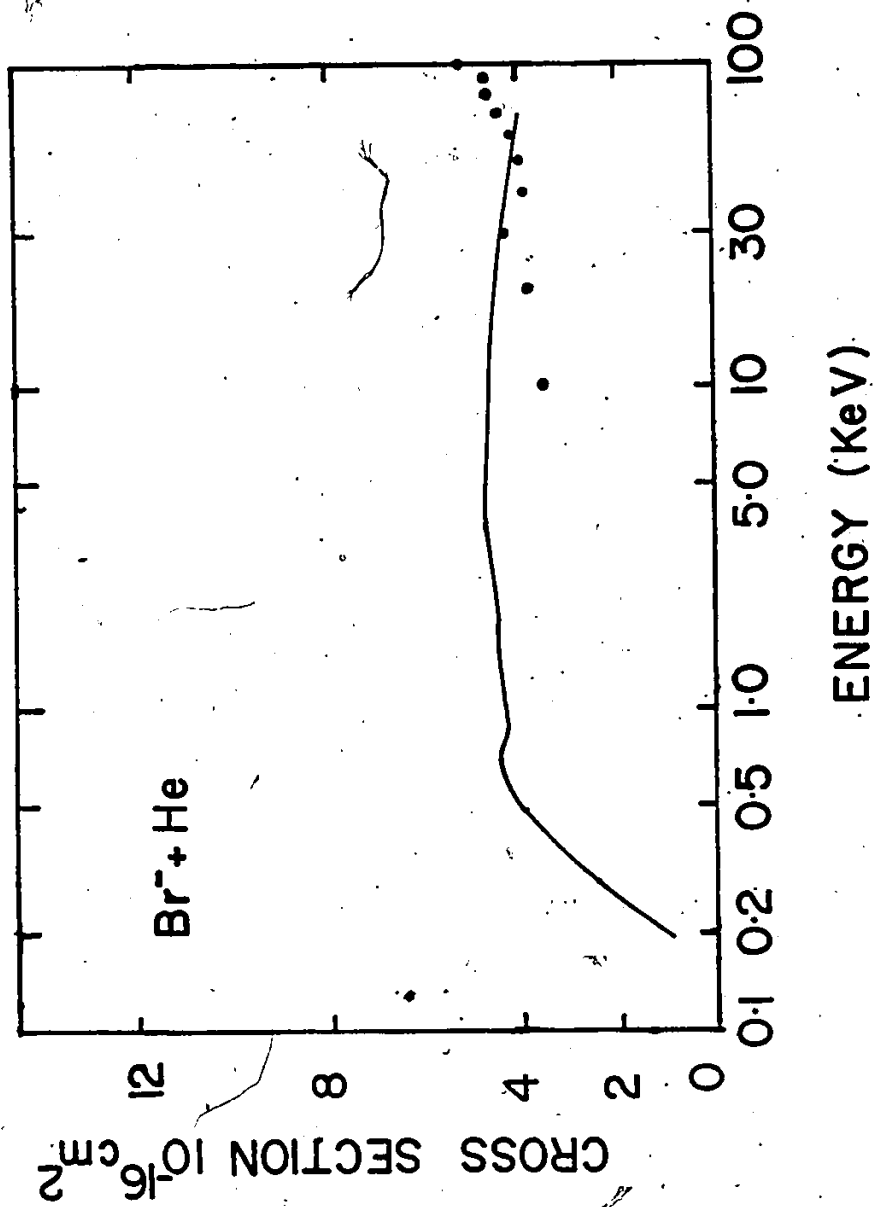


Fig. 11 Comparison between the Zero Range sudden approximation model of Gulyacq using the molecular energies of Olson and Liu, the present measurements shown by dots.

potentials. But it was found that for  $I^-$  ions colliding with the rare gases this behaviour was not present.

For  $Br^-$  ions colliding with the rare gases, it was found that " $\sigma_{-+}$ " behaves almost in between the behavior of  $F^-$ ,  $Cl^-$  and  $I^-$ .

A P P E N D I X  
-----

```

1.  SET ESC & ;#INM0          JUNE 1983
2.  ;THIS IS USED TO ENTER THE DIGITAL DATA FOR THE
3.  ;M0 CROSS SECTION LEAST SQUARES PROGRAM MORE EASILY.
4.  ;FOR INFORMATION REGARDING THE CONSTANTS ENTERED HERE
5.  ;SEE THE DOCUMENTATION FOR THE LEAST SQUARES PROGRAM #LSQRM0
6.  SET LENGTH 80
7.  SET NOLOG
8.  SET VALUE S0 '
9.  SET VALUE S9 '/*'
10. COMMENT TO END DATA ENTRY AFTER ONE LEAST SQUARES FIT ENTER ZERO FOR NM.
11. COMMENT TO END DATA ENTRY AFTER ALL LEAST SQUARES FITS ENTER ZERO FOR E.
12. READ VALUE W0 W1 W2 PROMPT 'E, T, SL,(3F10.5) ='
13. IF(W0 EQ 0) EXEC 51
14. SET VALUE S1 S0||W0
15. SET VALUE S1 SUBSTR(S1,SIZE(S1)-9)
16. SET VALUE S2 S0||W1
17. SET VALUE S2 SUBSTR(S2,SIZE(S2)-9)
18. SET VALUE S3 S0||W2
19. SET VALUE S3 SUBSTR(S3,SIZE(S3)-9)
20. READ STR S4 PROMPT 'TITLE,(12A4) ='
21. END &(S1||S2||S3||S4)
22. READ VAL W0 W1 W2 W3 W4 PROMPT 'SIG0M,SIG01,SIG02,SIGM1,SIG10,(5F10.5)='
23. SET VALUE S1 S0||W0
24. SET VALUE S1 SUBSTR(S1,SIZE(S1)-9)
25. SET VALUE S2 S0||W1
26. SET VALUE S2 SUBSTR(S2,SIZE(S2)-9)
27. SET VALUE S3 S0||W2
28. SET VALUE S3 SUBSTR(S3,SIZE(S3)-9)
29. SET VALUE S4 S0||W3
30. SET VALUE S4 SUBSTR(S4,SIZE(S4)-9)
31. SET VALUE S5 S0||W4
32. SET VALUE S5 SUBSTR(S5,SIZE(S5)-9)
33. END &(S1||S2||S3||S4||S5)
34. SET VALUE S5=''
35. SET VALUE N4=0
36. READ VALUE W0 N1 N2 PROMPT ' P, NM, N0 ,(F8.3,2I6)='
37. SET VALUE N4=N4+1
38. SET VALUE N7=N1+N2
39. IF(N7 EQ 0) EXEC 48
40. SET VALUE S1 S0||N1
41. SET VALUE S1 SUBSTR(S1,SIZE(S1)-5)
42. SET VALUE S3 S0||N2
43. SET VALUE S3 SUBSTR(S3,SIZE(S3)-5)
44. SET VALUE S4=S0||W0
45. SET VALUE S4 SUBSTR(S4,SIZE(S4)-7)
46. SET VALUE S5=S5||S1||S3||S4
47. IF(N4 LT 4) EXEC 36
48. END &S5
49. IF(N7 NE 0) EXEC 34
50. EXEC 11
51. END &S0
52. END &S9
53. SET ESCAPE ''

```

```

1. SET ESC & ;#INMP MAY 83
2. ;THIS IS USED TO ENTER THE DIGITAL DATA FOR THE
3. ;MP CROSS SECTION LEAST SQUARES PROGRAM MORE EASILY.
4. ;FOR INFORMATION REGARDING THE CONSTANTS ENTERED HERE
5. ;SEE THE DOCUMENTATION FOR THE LEAST SQUARES PROGRAM
6. SET LENGTH 80
7. SET NOLOG
8. SET VALUE S0 '
9. SET VALUE S9 '/*'
10. COMMENT TO END DATA ENTRY AFTER ONE LEAST SQUARES FIT ENTER ZERO FOR NM.
11. COMMENT TO END DATA ENTRY AFTER ALL LEAST SQUARES FITS ENTER ZERO FOR E.
12. READ VALUE W0 W1 W2 PROMPT 'E, T, SL =(3F10.5)'
13. IF (W0 EQ 0) EXEC 62
14. SET VALUE S1 S0||W0
15. SET VALUE S1 SUBSTR(S1,SIZE(S1)-9)
16. SET VALUE S2 S0||W1
17. SET VALUE S2 SUBSTR(S2,SIZE(S2)-9)
18. SET VALUE S3 S0||W2
19. SET VALUE S3 SUBSTR(S3,SIZE(S3)-9)
20. READ STR S4 PROMPT 'TITLE =(12A4)'
21. END &(S1||S2||S3||S4)
22. READ VAL W0 W1 W2 W3 W4 PROMPT 'SIG10,SIG1M,SIG12,SIGM0,SIG01=(5F10.3)'
23. SET VALUE S1 S0||W0
24. SET VALUE S1 SUBSTR(S1,SIZE(S1)-9)
25. SET VALUE S2 S0||W1
26. SET VALUE S2 SUBSTR(S2,SIZE(S2)-9)
27. SET VALUE S3 S0||W2
28. SET VALUE S3 SUBSTR(S3,SIZE(S3)-9)
29. SET VALUE S4 S0||W3
30. SET VALUE S4 SUBSTR(S4,SIZE(S4)-9)
31. SET VALUE S5 S0||W4
32. SET VALUE S5 SUBSTR(S5,SIZE(S5)-9)
33. END &(S1||S2||S4||S4||S5)
34. READ VALUE W0 W1 W2 W3 PROMPT 'BGM, BGP, D1, D2,(4F8.3)='
35. SET VALUE S1 S0||W0
36. SET VALUE S1 SUBSTR(S1,SIZE(S1)-7)
37. SET VALUE S2 S0||W1
38. SET VALUE S2 SUBSTR(S2,SIZE(S2)-7)
39. SET VALUE S3 S0||W2
40. SET VALUE S3 SUBSTR(S3,SIZE(S3)-7)
41. SET VALUE S4 S0||W3
42. SET VALUE S4 SUBSTR(S4,SIZE(S4)-7)
43. END &(S1||S2||S3||S4)
44. SET VALUE S5=''
45. SET VALUE N4=0
46. READ VALUE W0 N0 N1 PROMPT ' P(10**-3TORR)x,NM, NP ,(F8.3,2I6) ='
47. SET VALUE N7=N0+N1
48. IF (N7 EQ 0) EXEC 58
49. SET VALUE N4=N4+1
50. SET VALUE S1 S0||W0
51. SET VALUE S1 SUBSTR(S1,SIZE(S1)-7)
52. SET VALUE S2 S0||N0
53. SET VALUE S2 SUBSTR(S2,SIZE(S2)-5)
54. SET VALUE S3=S0||N1
55. SET VALUE S3 SUBSTR(S3,SIZE(S3)-5)
56. SET VALUE S5=S5||S2||S3||S1
57. IF (N4 LT 4) EXEC 46
58. END &S5
59. IF (N7 NE 0) EXEC 44
60. EXEC 11
61. END &S0
62. END &S9
63. SET ESCAPE ''

```

```

1. C LEAST SQUARES FIT TO (COUNT RATE RATIO/PRESSURE) #lsqrm0
2. C LINEAR FUNCTIONAL RELATION ASSUMED.
3. C *****SIGMA M0 CORRECTED - THIN TARGET CONDITION - *****
4. C TEMPERATURE AT WHICH THE EXPERIMENT HAS BEEN DONE : T ( K )
5. C ENERGY AT WHICH THE EXPERIMENT HAS BEEN DONE : E ( KEV )
6. C TARGET LENGTH = SL ( CM.)
7. C CROSS SECTION = SIGMA(1.E-15*(CM**2))
8. C PRESSURE = P = FP (E-3 TORR)
9. C
10. DIMENSION A(12,50),R(20),P(20),SR(20),I2(4),I1(4),FP(4),SIG0M(50),
11. &SIG01(50),SIG02(50),SIGM1(50),SIGI0(50),SIGM0(50),E(50),ESIGMA(50)
12. 15 L=1
13. READ(5,102) E(L),T,SL,(A(I,L),I=1,12)
14. 102 FORMAT(3F10.2,12A4)
15. IF(E(L).EQ.0.0) RETURN
16. 1 WRITE(6,103) E(L),T,SL,(A(I,L),I=1,12)
17. 103 FORMAT(1H1,30X,7H#LSQRM0/14H0 ENERGY = ,F5.1,24H KEV TEMPE
18. &RATURE = ,F6.2,17H K TARGET = ,F7.4,4H CM./1H0,12A4)
19. C READ THE TOTAL CROSS SECTIONS USED IN THE CORRECTION.
20. READ(5,109) SIG0M(L), SIG01(L), SIG02(L), SIGM1(L), SIGI0(L)
21. 109 FORMAT( 5F10.5 )
22. WRITE(6,110)SIG0M(L),SIG01(L),SIG02(L),SIGM1(L),SIGI0(L)
23. 110 FORMAT( 9H0 SIG0M=,F6.4,7H SIG01=,F6.4,7H SIG02=,F6.4
24. 1,7H SIGM1=,F6.4,7H SIGI0=,F8.4,13H (E-15 CM**2))
25. CSTE=4.8304*SL*(SIG0M(L)+SIG01(L)+SIG02(L)-SIGM1(L))/T
26. 105 FORMAT(4(2I6,F8.3))
27. M=0
28. C * RUN *
29. WRITE(6,104)
30. 104 FORMAT('0',58H IONS (-1) ATOMS (0) PRESSURE
31. IRATIO /45H (COUNTS) (COUNTS) (E-3 TORR)./ )
32. C COUNTS FOR NEGATIVELY CHARGED IONS : A2
33. C COUNTS FOR NEUTRAL ATOMS: A1
34. 11 READ(5,105) (I2(I),I1(I),FP(I),I=1,4)
35. DO 10 J=1,4
36. IF (I2(J).EQ.0) GO TO 30
37. M=M+1
38. A2=I2(J)
39. A1=I1(J)
40. R(M) = A1 / ( A2 + A1 / 2. )
41. IF (I1(J).EQ.0) A1=1.0
42. P(M)=FP(J)
43. IF (M.EQ.1) P(Z)=P(1)
44. P(M)=P(M)-P(Z)
45. SR(M)=R(M)*R(M)*(1./A1+1./A2)
46. WRITE(6,106) A2, A1, P(M), R(M)
47. 106 FORMAT(1H ,5X,F10.0,5X,F10.0,5X,F10.3,5X,F10.8)
48. 10 CONTINUE
49. GO TO 11
50. C
51. 30 DO 14 K=1,3
52. IF(K.EQ.1)WRITE(6,101)
53. 101 FORMAT(31H0NO TARGET THICKNESS CORRECTION)
54. IF(K.EQ.2) WRITE(6,112)
55. 112 FORMAT(31H0CORRECTED FOR TARGET THICKNESS)

```

```

56.      IF(K.EQ.3) WRITE(6,111)
57. 111 FORMAT(54H0CORRECTED FOR TARGET THICKNESS AND BEAM GAS THICKNESS)
58.      C      K IS THE NUMBER OF THE CORRECTION.
59.      SW = 0.
60.      X = 0.
61.      Y = 0.
62.      YY=0.
63.      XX = 0.
64.      XY = 0.
65.      C      J IS THE NUMBER OF THE RUN.
66.      DO 16 J=1,M
67.      C      VALUE OF THE SLOPE, METHOD OF LINEAR LEAST SQUARE FIT
68.      C      AND ITS ERROR
69.      C      X,Y,XX,XY ARE WEIGHTED MEAN VALUES.
70.      IF(SR(J).EQ.0) SR(J)=1.0
71.      W=1./SR(J)
72.      SW=SW + W
73.      X=X+P(J)*W
74.      Y=Y+R(J)*W
75.      XX=XX+P(J)*P(J)*W
76.      XY=XY+P(J)*R(J)*W
77.      YY=YY+R(J)*R(J)*W
78. 16 CONTINUE
79.      C
80.      C      ERROR=SLOPE ERROR FROM INDIVIDUAL POINTS
81.      ERROR=1./SQRT(XX-X*X/SW)
82.      X=X/SW
83.      Y=Y/SW
84.      XX=XX/SW
85.      XY=XY/SW
86.      YY=YY/SW
87.      SLOPE = (XY-X*Y)/(XX-X*X)
88.      C      ERR=SLOPE ERROR FROM SPREAD OF POINTS FROM LINE
89.      ERR=1.E+3*SQRT(SLOPE*((YY-Y*Y)/(XY-X*Y)-SLOPE)/M)
90.      C      INTERCEPT +/- ERROR IN INTERCEPT = CEPT +/- ERCEPT.
91.      CEPT=Y-X*SLOPE
92.      ERCEPT=ERROR*SQRT(XX)
93.      ERROR=ERROR*1.0E+3
94.      SLOPE=SLOPE*1.0E+3
95.      SIGMA =1.0351E-19*T*SLOPE/SL
96.      SIGM0(L)=SIGMA*1.0E15
97.      ERSIG=SIGMA*ERROR/SLOPE
98.      ESIGMA(L)=ERSIG*1.0E15
99.      SIGP=SIGMA+ERSIG
100.     SIGM=SIGMA-ERSIG
101.     WRITE(6,108)SLOPE,ERROR,CEPT,ERCEPT,ERR,SIGP,SIGMA,ERSIG,E(L),SIGM
102. 108 FORMAT(20H0 EQU. FOR BEST LINE/11H RATIO = (,F10.5,3H+/-,F8.5,14H
103. &)*PRESSURE + (,F10.5,3H+/-,F10.5,2H)./
104. &30H0 SLOPE ERROR FROM LINE FIT = ,F10.5/T40,1PE11.4/
105. &25H TOTAL CROSS SECTION = (,1PE11.4,3H+/-,E11.4,12H) CM**2 AT,0
106. &PF6.1,4H KEV/T40,1PE11.4/)
107.     DO 14 J=1,M
108.     GO TO (12,13,14),K
109.      C      CORRECTED MEAN RATIO - TARGET THICKNESS CORRECTION -.
110. 13 R(J)=R(J)/(1.+(CSTE-SIGM1(L)*SIG10(L)/SIGMA*4.8303E-15*SL/T)*P(J))

```

```

111.      P(J)=P(J)+1.E+3*CEPT/SLOPE
112.      12 R(J)=R(J)*(1.+(CSTE-SIGM1(L)*SIG10(L)/SIGMA*4.8303E-15*SL/T)*P(J))
113.      14 CONTINUE
114.      WRITE(6,113)
115.      113 FORMAT(120H _____)
116.      & _____)
117.      L=L+1
118.      READ(5,102) E(L),T,SL,(A(I,L),I=1,12)
119.      C GOING TO ANOTHER EXPERIMENT?
120.      IF(E(L).NE.0.0) GO TO 1
121.      WRITE(6,114)
122.      L=L-1
123.      114 FORMAT(80H1|ENERGY SIG0M SIG01 SIG02 SIGM1 SIG10 SIGM0
124.      & ERROR UPPER LOWER)
125.      DO 115 I=1,L.
126.      SIGP=SIGM0(I)+ESIGMA(I)
127.      SIGM=SIGM0(I)-ESIGMA(I)
128.      115 WRITE(6,116)E(I),SIG0M(I),SIG01(I),SIG02(I),SIGM1(I),SIG10(I),SIGM
129.      &0(I),ESIGMA(I),SIGP,SIGM,(A(J,I),J=1,12)
130.      116 FORMAT(2H |,F6.1,5F8.3,F10.5,3F8.5,12A4)
131.      WRITE(6,117)
132.      117 FORMAT(120H | _____)
133.      & _____)
134.      GO TO 15
135.      17 RETURN
136.      END
137.      //GO.SYSIN DD *

```

```

1. C LEAST SQUARES FIT TO (COUNT RATE RATIO/PRESSURE). #LSQMP may 83
2. C LINEAR FUNCTIONAL RELATION ASSUMED.
3. C ***** SIGMA MP CORRECTED - THIN TARGET CONDITION - *****
4. C BG = BACKGROUND TO COUNTS
5. C DBG = ERROR ON BACKGROUND COUNTS.
6. C TEMPERATURE AT WHICH THE EXPERIMENT HAS BEEN DONE : T ( K )
7. C ENERGY AT WHICH THE EXPERIMENT HAS BEEN DONE : E ( KEV )
8. C TARGET LENGTH = SL ( CM.)
9. C CROSS SECTION = SIGMA(1.E-15*(CM**2))
10. C PRESSURE = P = FP (E-3 TORR)
11. C
12. DIMENSION A(12,99),R(20),P(20),SR(20),I2(4),I1(4),FP(4),SIG10(99),
13. &SIG1M(99),SIG12(99),SIGM0(99),SIG01(99),SIGMP(99),E(99),ESIGMA(99)
14. 1,BGM(99),BGP(99),DBM(99),DBP(99)
15. 15 L=1
16. READ(5,102) E(L),T,SL,(A(I,L),I=1,12)
17. IF(E(L).EQ.0.0) RETURN
18. 102 FORMAT(3F10.2,12A4)
19. 1 WRITE(6,103) E(L),T,SL,(A(I,L),I=1,12)
20. 103 FORMAT(14H1 ENERGY = ,F5.1,24H KEV TEMPERATURE = ,F6.2,
21. 17H K TARGET = ,F7.4,4H CM.,12A4/1H ,30X,7H#LSQMP)
22. C READ THE TOTAL CROSS SECTIONS USED IN THE CORRECTION.
23. READ(5,109) SIG10(L),SIG1M(L),SIG12(L),SIGM0(L),SIG01(L)
24. 109 FORMAT( 5F10.5 )
25. WRITE(6,110)SIG10(L),SIG1M(L),SIG12(L),SIGM0(L),SIG01(L)
26. 110 FORMAT( 9H0 SIG10=,F8.4,7H SIG1M=,F6.4,7H SIG12=F6.4
27. 1,7H SIGM0=,F6.4,7H SIG01=,F6.4,13H (E-15 CM**2))
28. CSTE=4.8304*SL*(SIG10(L)+SIG1M(L)+SIG12(L)-SIGM0(L))/T
29. 105 FORMAT(4(I6,I6,F8.3))
30. READ(5,107) BGM(L),BGP(L),DBM(L),DBP(L)
31. 107 FORMAT( 4F8.3 )
32. WRITE(6,118)BGM(L),BGP(L),DBM(L),DBP(L)
33. 118 FORMAT( 7H BGM=,F8.3,7H BGP=,F8.3,
34. 17H DBM=,F8.3,7H DBP=,F8.3)
35. M=0
36. C * RUN *
37. WRITE(6,104)
38. 104 FORMAT('0',58H IONS -1 IONS +1 PRESSURE
39. 1RATIO /45H (COUNTS) (COUNTS) (E-3 TORR)./)
40. C COUNTS FOR NEGATIVELY CHARGED IONS : A2-BGM(L)
41. C COUNTS FOR POSITIVE CHARGED IONS: A1-BGP(L)
42. 11 READ(5,105)(I2(I),I1(I),FP(I),I=1,4)
43. DO 10 J=1,4
44. IF(I2(J).EQ.0) GO TO 30
45. M=M+1
46. A2=I2(J)
47. A1=I1(J)
48. A3=A2-BGM(L)
49. A4=A1-BGP(L)
50. R(M) = A4 / ( A3 + A4 / 2. )
51. IF(A1.EQ.BGP(L)) A4=1.0
52. P(M)=FP(J)
53. IF(M.EQ.1) P(Z)=P(1)
54. P(M)=P(M)-P(Z)
55. SR(M)=R(M)*R(M)*((A1+DBP(L))*DBP(L))/A4/A4 +(SQRT(A2+DBM(L))*DBM(L)

```

```

56.      1  )+.5*SQRT(A1+DBP(L)*DBP(L))**2/(A3+.5*A4)**2)
57.      WRITE(6,106) A2, A1, P(M), R(M)
58. 106  FORMAT(1H ,5X,F10.2,5X,F10.2,5X,F10.3,5X,F15.8)
59.      10 CONTINUE
60.      GO TO 11
61.  C
62.      30 DO 14 K=1,3
63.      IF(K.EQ.1)WRITE(6,101)
64. 101  FORMAT(31H0NO TARGET THICKNESS CORRECTION)
65.      IF(K.EQ.2) WRITE(6,112)
66. 112  FORMAT(31H0CORRECTED FOR TARGET THICKNESS)
67.      IF(K.EQ.3) WRITE(6,111)
68. 111  FORMAT(54H0CORRECTED FOR TARGET THICKNESS AND BEAM GAS THICKNESS)
69.  C   K IS THE NUMBER OF THE CORRECTION.
70.      SW = 0.
71.      X = 0.
72.      Y = 0.
73.      YY=0.
74.      XX = 0.
75.      XY = 0.
76.  C   J IS THE NUMBER OF THE RUN.
77.      DO 16 J=1,M
78.  C   VALUE OF THE SLOPE, METHOD OF LINEAR LEAST SQUARE FIT
79.  C   AND ITS ERROR
80.  C   X,Y,XX,XY ARE WEIGHTED MEAN VALUES.
81.      IF(SR(J).EQ.0) SR(J)=1.0
82.      W=1./SR(J)
83.      SW=SW + W
84.      X=X+P(J)*W
85.      Y=Y+R(J)*W
86.      XX=XX+P(J)*P(J)*W
87.      XY=XY+P(J)*R(J)*W
88.      YY=YY+R(J)*R(J)*W
89.      16 CONTINUE
90.  C
91.  C   ERROR=SLOPE ERROR FROM INDIVIDUAL POINTS
92.      ERROR=1./SQRT(XX-X*X/SW)
93.      X=X/SW
94.      Y=Y/SW
95.      XX=XX/SW
96.      XY=XY/SW
97.      YY=YY/SW
98.      SLOPE = (XY-X*Y)/(XX-X*X)
99.  G   ERR=SLOPE ERROR FROM SPREAD OF POINTS FROM LINE
100.      ERR=1.E+3*SQRT(SLOPE*((YY-Y*Y)/(XY-X*Y)-SLOPE)/M)
101.  C   INTERCEPT +/- ERROR IN INTERCEPT = CEPT +/- ERCEPT.
102.      CEPT=Y-X*SLOPE
103.      ERCEPT=ERROR*SQRT(XX)
104.      ERRQR=ERROR*1.0E+3
105.      SLOPE=SLOPE*1.0E+3
106.      SIGMA =1.0351E-19*T*SLOPE/SL
107.      SIGMP(L)=SIGMA*1.0E15
108.      ERSIG=SIGMA*ERROR/SLOPE
109.      ESIGMA(L)=ERSIG*1.0E15
110.      SIGP=SIGMA+ERSIG


```

```

111.      SIGM=SIGMA-ERSIG
112.      WRITE (6,108) SLOPE,ERROR,CEPT,ERCEPT,ERR,SIGP,SIGMA,ERSIG,E(L),
113.      &SIGM
114.      108 FORMAT(20H0 EQU. FOR BEST LINE/11H RATIO = (,F12.5,3H+/-,F15.5,14
115.      &H)*PRESSURE + (,F10.5,3H+/-,F10.5,2H)./
116.      &30H0 SLOPE ERROR FROM LINE FIT = ,F10.5/T40,1PE11.4/
117.      &25H TOTAL CROSS SECTION = (,1PE11.4,3H+/-,E11.4,12H) CM**2 AT,0
118.      &PF6.1,4H KEV/T40,1PE11.4/)
119.      DO 14 J=1,M
120.      GO TO (12,13,14),K
121.      C CORRECTED MEAN RATIO - TARGET THICKNESS CORRECTION -.
122.      12 R(J)=R(J)*(1.+(CSTE-SIGM0(L)*SIG01(L)/SIGMA*4.8303E-15*SL/T)*P(J))
123.      GO TO 14
124.      13 R(J)=R(J)/(1.+(CSTE-SIGM0(L)*SIG01(L)/SIGMA*4.8303E-15*SL/T)*P(J))
125.      P(J)=P(J)+1.E+3*CEPT/SLOPE
126.      R(J)=R(J)*(1.+(CSTE-SIGM0(L)*SIG01(L)/SIGMA*4.8303E-15*SL/T)*P(J))
127.      14 CONTINUE
128.      WRITE (6,113)
129.      113 FORMAT(120H _____)
130.      &_____
131.      L=L+1
132.      READ(5,102) E(L),T,SL,(A(I,L),I=1,12)
133.      C GOING TO ANOTHER EXPERIMENT?
134.      IF (E(L).NE.0.0) GO TO 1
135.      WRITE (6,114)
136.      L=L-1
137.      114 FORMAT(80H1|ENERGY SIG10 SIG1M SIG12 SIGM0 SIG01 SIGMP
138.      & ERROR UPPER LOWER)
139.      DO 115 I=1,L
140.      SIGP=SIGMP(I)+ESIGMA(I)
141.      SIGM=SIGMP(I)-ESIGMA(I)
142.      115 WRITE (6,116) E(I),SIG10(I),SIG1M(I),SIG12(I),SIGM0(I),SIG01(I),SIGM
143.      &P(I),ESIGMA(I),SIGP,SIGM,(A(J,I),J=1,12)
144.      116 FORMAT(2H |,F6.1,5F8.3,F10.5,3F8.5,12A4)
145.      WRITE (6,117)
146.      117 FORMAT(120H |_____
147.      &_____
148.      GO TO 15
149.      17 RETURN
150.      END
151.      //GO.SYSIN DD *

```

## REFERENCES

1. Massey, H.S.W., and Burhop, E.H.S.  
Electronic and Ionic Impact Phenomena, (Oxford: Clarendon Press), (1952).
2. V.M. Dukel'skii and N.V. Fedorenko.  
Sov. Physics-JETP, (2), 307, (1956).
3. M. Matic and B. Cobic.   
J. Physics B, (4), 111, (1971).
4. I.U.F. Bydin and V.M. Dukel'skii.  
Sov. Physics-JETP, (4), 474, (1957).
5. W.J. Lichtenberg, K. Bethge and H. Schmidt-Bocking.  
J. Physics B, (13), 343, (1980).
6. B. Hird and F. Rahman.  
Physical Review A, (26), 3108, (1982).
7. B. Hird and F. Rahman.  
Physical Review A, (29), 1541, (1984).
8. B. Hird and F. Rahman.  
 $I^-$  ions in rare gases, Submitted for publication.
9. B. Hird and F. Rahman.  
Canadian J. Physics, (62), 544, (1984).
10. YU.N. Demkov.  
Sov. Physics-JETP, (19), 762, (1964).
11. A.Z. Devdariani.  
Sov. Physics Tech. Phys. (18), 255, (1973).

12. J.P. Gauyacq.  
J. Physics B, (12), 13, (1979).
13. Champion and Doverspike.  
Physical Review A, (13), 609, (1976).
14. Fricke, Muller and Salzborn.  
Nuc. Inst. and Method, 175, 379, (1980).
15. Hans D.Betz, G.Ryding and A.B.Wittkower.  
Physical Review A, (3), 197, (1971).
16. Nikolaev, Dmitriev, Fateva and Teplova.  
Sov. Physics-JETP, (13), 695, (1961).
17. Negative Ions.  
By: B.M. Smirnov, P.72.
18. R.E. Olson and B.Liu.  
Physical Review A, (20), 1344, (1979).

.....